High-precision Sediment Tracking for Characterization of Sediment Transport of a Rural Stream in Southern Ontario Conditioned by Glacial Legacy Deposits

by

Aryn Cain

A thesis

presented to the University of Waterloo

in fulfillment of the

thesis requirement for the degree of

Master of Applied Science

in

Civil Engineering

Waterloo, Ontario, Canada, 2019

Author's Declaration

I hereby declare that I am the sole author of this thesis. This is a true copy of the thesis, including any required final revisions, as accepted by my examiners.

I understand that my thesis may be made electronically available to the public.

Abstract

Semi-alluvial rivers are common in Southern Ontario and are characterized by sections of exposed highly consolidated glacial till and other sections of mobile sediment. Such rivers are typically characterized by a series of downstream fining trends (sediment links) as a result of the discontinuous distribution of sediment sources. Evolutionary models have been presented that describe these streams and tend focus on the feedback between river morphology, hydraulics and sediment transport. Sediment transport that occurs on the channel bed is the most important component for understanding this feedback and is typically quantified using bulk sampling, indirect sampling or sediment tracking. All of these methods are useful but also miss important details of the process such as active width and burial depth. This methodological deficiency was used as motivation for the development of a new type of Radio Frequency Identification tracer ("wobblestone") that has the potential for increased tracer recovery rates and the assessment of tracer burial depth.

The goal of this thesis is to demonstrate the effectiveness of this new high-precision tracking technology and to characterize the sediment regime of a rural semi-alluvial glacial till river. The first goal was accomplished by developing a methodology to determine the burial depth of tracers and testing this method in both the lab and field setting. The second objective was achieved by measuring the longitudinal profile, identifying the location of sediment links and sediment tracking using the newly developed wobblestones at a field site located on the western branch of Ganatsekiagon Creek in Pickering, Ontario. Ganatsekiagon Creek is a semi-alluvial river that is of interest because in the next 5 years its watershed will see a rapid increase in urban-residential land-use (from 2% to 43%). The site has also been identified as an important habitat for Redside Dace, an endangered species in Canada, which makes it important for research partners such as the Toronto Region Conservation Authority, who are responsible for managing the watershed.

Wobblestones show potential as a new sediment tracking technology that can determine the burial depth of stones and increase the recovery rates of tracers. Field tests indicated improved recovery rates and that the burial depth can be determined with an accuracy of +/- 4 cm. Additional fieldwork should be conducted in order to confirm the accuracy of the burial depth measurements. In addition, flume investigations should be conducted to determine the mobility difference between wobble and non-wobblestones.

Two sediment links have been identified on the western branch of Ganatsekiagon Creek. The field tracer results show that the gradients of bed slope and particle size lead to significant differences in sediment dynamics over short distances along the river. In addition, the results supported the hypothesis that the upstream site is a source of bedload and that this reach may be sensitive to hydrologic changes in the watershed as a result of the ongoing urbanization. The study site should remain the focus of future monitoring in order to verify the apparent differences in the mobility and transport through these semi-alluvial glacial till rivers and to assess their sensitivity and evolution as a result of urbanization.

Acknowledgements

I would first like to acknowledge that the University of Waterloo is located on land promised to the Six Nations of the Grand River as part of the Haldimand Tract and is located within the traditional territory of the Neutral, Anishinaabeg and Haudenosaunee peoples. In addition, the study sites for this thesis are within the traditional territory of the Anishinabewaki, Huron-Wendat and Haudenosaunee peoples.

I would like to thank my supervisor, Dr. Bruce MacVicar for his continuous support and guidance throughout my Master's Degree, as well as Elli Papangelakis for her mentorship and help with both field work and thesis editing. Thank you to Kayla Goguen, Panos Papangelakis, Matt Iannetta, Adam Schneider, Chris Muirhead, Steven Meyer, Jackie Wintermeyer and Louis Vervynck for their help in the lab and in the field. This thesis would not be where it is today without their blood, sweat and tears.

Financial support for this thesis was provided by Natural Sciences and Engineering Research Council of Canada (NSERC) Strategic Grant (463321): Assessing and Restoring the Resilience of Urban Stream Networks presented to Dr. MacVicar.

Lastly, I would like to thank all my friends and family for their unconditional love and support over the past two years. I wouldn't have made it this far without them and I am forever grateful to have such an amazing group of people in my corner.

Table of Contents

List of Figures

List of Tables

Chapter 1 - Introduction

River systems convey both sediment and water through a watershed from upstream sources to a downstream outlet. As the supply of sediment and water fluctuates, the river bed will typically go through phases of degradation and aggradation until the system reaches an equilibrium state (Lane 1954). Changes to the watershed such as urbanization can cause large scale degradation or aggradation of the river as it adjusts to a new equilibrium state. Several predictive model use sediment transport as an input to understand the current and future evolutionary states of rivers under various conditions, including urbanization. The most commonly used model was presented by Mackin (1948) and is known as the graded river. A graded river will continually try to adjust its longitudinal profile in order to reach a balanced state where the water velocity is equal to the velocity required to transport the supplied material, under prevailing channel conditions and available discharge (Mackin 1948). Rivers typically have longitudinal profiles that decrease in slope in the downstream direction and exhibit downstream fining of bed material due decreasing flows, shear stress and stream power as a result of this decrease in slope.

Semi-alluvial rivers are common in Southern Ontario and are characterized by sections of exposed bedrock (typically a highly consolidated glacial till) and other sections of mobile sediment. The mobile sediment is typically introduced from upstream sources, tributaries or through the erosion of the bedrock. Since most semi-alluvial glacial till rivers in Southern Ontario don't have steep headwaters (Phillips and Desloges 2015b), the majority of the sediment originates from bed and bank erosion of glacial deposits (Gallagher, Balme, and Clifford 2017; Phillips and Desloges 2015b; Rice and Church 1998; Thayer et al. 2016). This results in a large variety of grain sizes and a discontinuous distribution of sediment due to the erratic lateral sediment sources (Phillips and Desloges 2015b; Rice and Church 1998; Thayer et al. 2016). Studies have identified areas of localized downstream fining, that are characterized by steep upstream sections with coarse material and downstream flatter sections with finer material (Phillips & Desloges, 2015b; Rice & Church, 1998; Thayer et al., 2016). These sections are commonly referred to as sediment links, with

transitions between links characterized by local convex slopes that indicate a source for the supply of coarse bed material.

Since most of the current evolutionary models focus on the feedback between river morphology, hydraulics and sediment transport, it is important that these variables are quantifiable in real rivers (not just lab settings). This thesis focuses on the characterization of sediment transport through quantifying bedload transport rates. Bedload transport is described as the solid larger inorganic material that either rolls, slides or saltates within a few grain diameters of the stream bed (Dingman 2009). There are three main methods for quantifying bedload transport: bulk sampling, indirect sampling and sediment tracking. Unfortunately, none of the above methods can fully quantify the rate of bedload transport as they are all missing different aspects of the process. Existing methodological deficiencies were used as motivation for the development of a new type of Radio Frequency Identification (RFID) tracer called a 'wobblestone' (Papangelakis et al. 2019). This tracer is advantageous because it ensures that the orientation of the RFID transponder is always the same despite any rotation of the tracer stone. This allows the precise positioning of the tracer in the horizontal plane (± 5 cm) and, for the first time with RFID tracers, the estimation of the burial depth. However, this new tracer has only been tested in the lab, and an opportunity exists to demonstrate its effectiveness for the first time in a field study.

The aim of the field study is to characterize the current state of a rural stream in southern Ontario at a moment just prior to its urbanization. Wobblestones have been tested for the first time in the field as part of this thesis. The selected field site is the western branch of Ganatsekiagon Creek, a tributary of Duffins Creek in Pickering, Ontario. The site is of interest because the next 5 years will see a rapid increase in urban-residential land-use (from 2% to 43%) as a result of the Seaton Lands Development. Such a land-use chance will significantly alter the current channel morphology, hydrology and stream power. The chosen site has an underlying geology of primarily Halton Till and Newmarket Till which causes the system to be semi-alluvial in nature. The site has also been identified as an important habitat for Redside Dace,

an endangered species in Canada, which makes it important for research partners such as the Toronto Region Conservation Authority, who are responsible for managing the watershed. Specific objectives of this thesis are to;

i) Demonstrate and assess the effectiveness and precision of the high-precision bedload transport tracking technique that uses the newly developed 'wobblestones', and

ii) Characterize the sediment regime of a rural semi-alluvial glacial till river.

The sediment regime will be characterized by measuring the longitudinal profile, identifying sediment links, and sediment tracking. Earlier fieldwork in the research group on lower branches of Ganatsekiagon Creek will be used as a point of comparison during the analysis of the study area.

The organization of this thesis is as follows. Chapter 2 will provide background information on sediment transport, methods for quantifying bedload transport, river longitudinal profiles and river evolution models. Chapters 3 and 4 present the methods and results relating to the first and second objectives of the study. Chapter 5 presents the conclusions of this study, recommends future steps and identifies potential future areas of research.

Chapter 2 - Literature Review

The following sections provide a background for this thesis and identifies the research gaps that will be addressed in Chapters 3 and 4. First, general sediment transport theory is introduced and methods for measuring bedload transport are reviewed to support the first research gap, which is methodological in nature. Second, river longitudinal profiles are discussed and literature relating to equilibrium states of the longitudinal profiles are reviewed to support the second research gap related to expected impact of urbanization and the need for a baseline study on transition points between sediment links in a longitudinal river profile.

2.1 Sediment Transport

Sediment transport describes the movement of particles in riverine, aeolian, costal and terrestrial environments. Total load accounts for everything that is being transported by a system including inorganic material, organic material, and dissolved gases (Figure 1). Inorganic material can be sub-classified into the particulate load and dissolved load (ions such as calcium or magnesium) (Figure 1). The particulate load is commonly referred to as total sediment transport which can then be further divided into the wash load, which is very small material that remains suspended even during very low flows, and bed-material load which is the movement of material that makes up the bed (Figure 1 & Figure 2). Bed-material transport is divided into two main categories: bedload transport and suspended sediment transport. Suspended sediment moves with fluid turbulence and typically travels at a height of several grain sizes above the bed, while bedload transport maintains intermittent contact with the bed and typically rolls, slides or saltates (Figure 2) within a few grain diameters of the stream bottom (Dingman 2009).

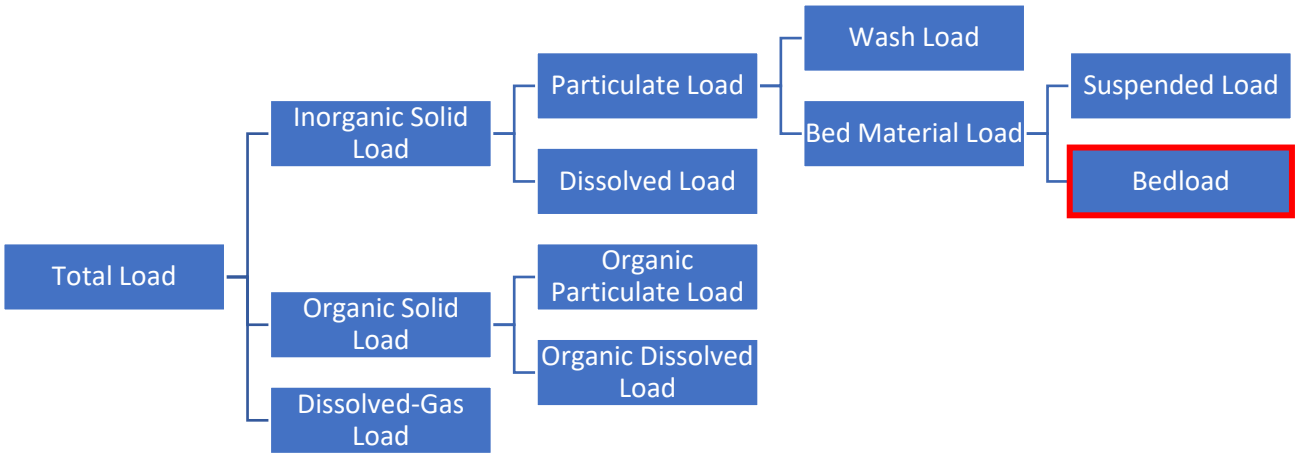

Figure 1 - Total transport. Modified from: Dingman (2009)

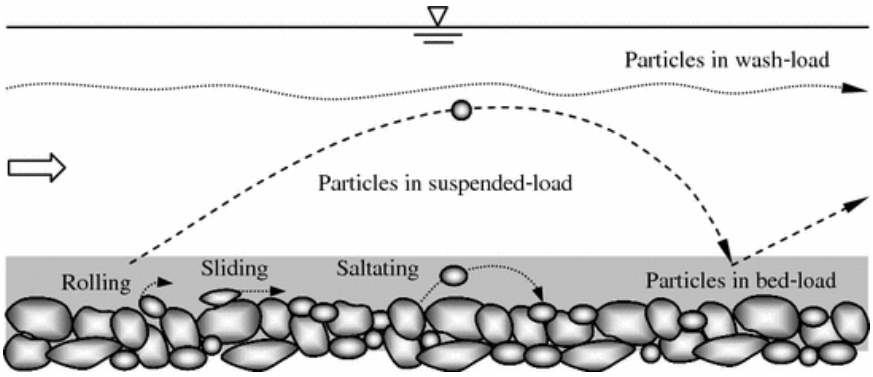

Figure 2 - Forms of total sediment transport. Figure from: *Dey (2014)*.

The total bedload transport rate (Q_s) can be calculated based on the following equation [m^3/year]:

$$Q_s = V_b D_s W_s (1 - P) \quad (1)$$

where V_b is the average or virtual rate of the transported material [m/year], P is the porosity of the bed material [-], D_s is the depth the active transport layer [m] and W_s is the width of the active transport layer [m] (Hassan, Church, and Ashworth 1992).

Du Boys (1987) published one of the first empirical formulas that describes bedload transport:

$$q_s = \kappa_D \cdot \tau_o \cdot (\tau_o - \tau_{cr}), \tau_o > \tau_{cr} \quad (2)$$

where q_s, κ_D, τ_o, and τ_o, are the bedload transport per unit width of the channel [m^2/year], a constant that is dependent on grain size, the bed shear stress [N/m^2], and the critical shear stress [N/m^2], respectively

(Du Boys 1879). However, Du Boys (1879) assumed that bedload material moves as a series of layers as opposed to individual grains (Ettema and Mutel 2004).

Several researchers tried to further the understanding of bedload transport by studying the movement of how coarse sand and fine gravel move in laboratory flumes. Shields (1936) introduced two dimensionless parameters that are still commonly used today to describe incipient motion of bed material. The first parameter, dimensionless shear stress (τ_*), is a ratio between the two forces acting on a particle; the total erosion force (F_E) and the gravitational force (F_G) (Dingman 2009):

$$\frac{F_E}{F_G} \propto \frac{\rho \cdot {\mu_*}^2 \cdot {d_p}^2}{(\rho_s - \rho) \cdot g \cdot {d_p}^3} = \frac{\rho \cdot {u_*}^2}{(\rho_s - \rho) \cdot g \cdot d_p} = \frac{\tau_o}{(\gamma_s - \gamma) \cdot d_p} \equiv \tau_* \tag{3}$$

where ρ, ρ_s, u_*, g, d_p, Υ, and Υ_s are the fluid mass density [Kg/m^3], sediment mass density [Kg/m^3], friction velocity [m/s], the acceleration due to gravity [m/s^2], particle diameter [m], fluid weight density [N/m^3], and the particle weight density [N/m^3], respectively (Shields 1936). Shields (1936) conducted a series of experiments using a uniform bed that related τ_* to his second dimensionless parameter; boundary Reynolds Number (Re_*):

$$\mathrm{Re}_* \equiv \frac{\mathrm{u}_* \cdot \mathrm{d_p}}{\eta} \tag{4}$$

where η is the kinematic viscosity of the fluid [m^2/s]. Re_* physically represents the ratio of the height of the roughness to the height of the hydraulically smooth viscous sub-layer. If Re_* is greater than 5, the particles that make up the roughness extend past the viscous sub-layer and the flow is considered transitional or rough (Figure 3). Shields (1936) conducted a series of flume experiments that analyzed the incipient motion of various sizes of particles and the corresponding τ_*. The threshold or critical dimensionless shear stress (τ_{*c}) that caused incipient motion of the particle was then plotted versus the boundary Reynolds number (Figure 3) and is known as the Shields Diagram.

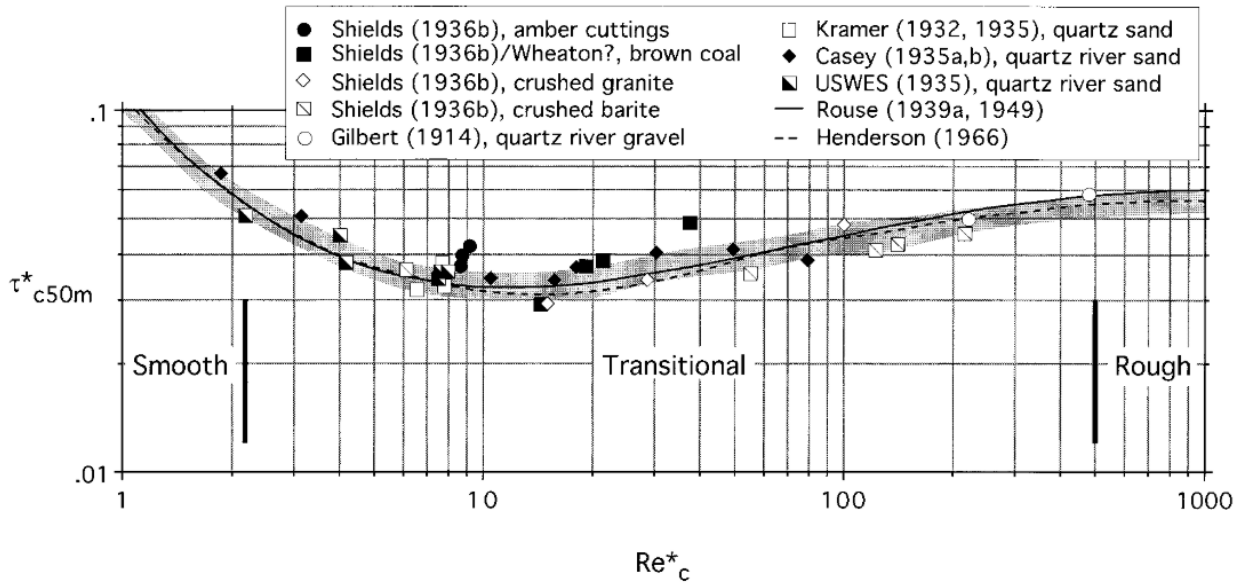

Figure 3 – Shields Diagram. Figure from *Buffington (2000)*

If τ_* is greater than the threshold (Figure 3), then the τ_* is enough to create motion, if $\tau_*$is below the line then the τ_* is not large enough to cause motion (Dingman 2009). Hjulström (1939) released an alternative method for estimating particle mobility that relates d_p to the mean velocity required to initiate motion (U) (Figure 4). He also added a second line that separates transportation and deposition, this relationship is based on the principle that once the motion of a particle begins it will stay mobile until the velocity is decreased past 2/3 of the critical velocity (U_c) (Dingman 2009).

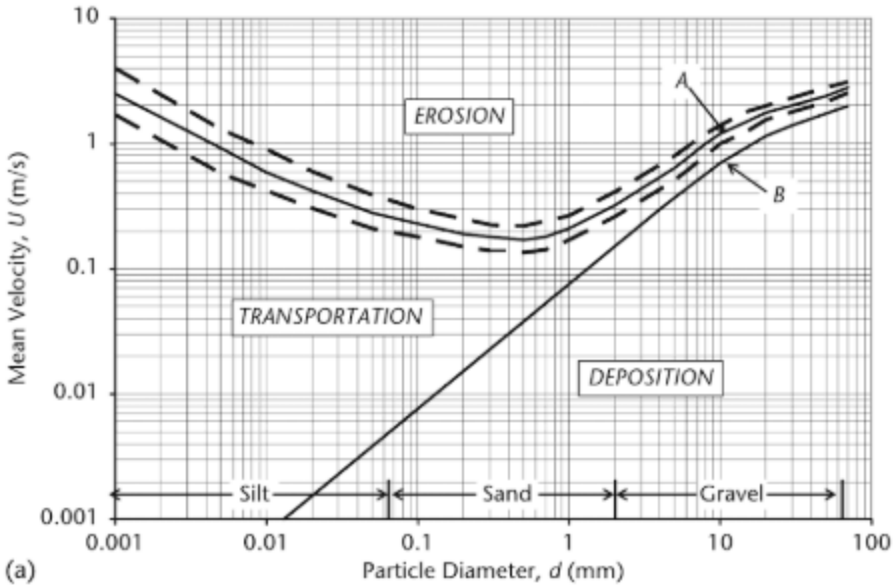

Figure 4 - Relation between mean velocity and particle diameter. Figure from Dingman (2009)

Several researchers over the years have reproduced the Shields diagram using different data sources from both flume and field experiments. Dade and Friend (1998) showed by plotting both lab (from Leopold and Wolman (1957)) and field data from alluvial rivers, that natural river systems don't always achieve the same threshold Shields parameters as the lab results (Figure 5).

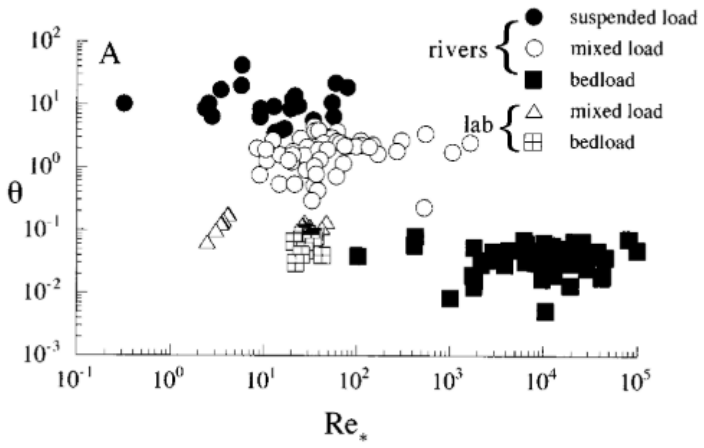

Figure 5 – Shields diagram compared to lab and field data. Figure From *Dade and Friend (1998)*

Further, most sediment transport models only apply for a small subset of conditions under which they were derived. For example the commonly used Meyer-Peter Muller formula for bedload transport can only be applied to rivers that experience low to moderate transport rates of gravel (Wilcock and Crowe

2003). Due to this, several equations relating sediment transport rates to various flow metrics and channel characterises have been derived under a variety of conditions (Dingman 2009).

2.1.1 Stream Power

Bagnold (1966) introduced a new parameter to predict sediment transport characteristics of a river: available stream power (Bagnold 1966). Stream power (Ω) can be thought of as the potential energy that moving water has to perform geomorphic work or sediment transport per unit length of the stream (Phillips and Desloges 2014):

$$\Omega = \gamma Q S \tag{5}$$

where S and Q are the channel slope and flow rate, respectively. Stream power can then be divided by width (w) and is referred to as specific stream power (ω):

$$\omega = \frac{\gamma Q S}{w} \tag{6}$$

Church (2002) demonstrated that since bedload transport rate is directly related to stream flow and slope it can be said that bedload transport is proportional to stream power. This is further explained in Section 2.3.

2.2 Measuring Bedload Transport

Sediment transport is a key process for understanding how riverine systems work and for predicting how they will adjust to various changes. Thus, being able to quantitatively describe sediment transport is a fundamental requirement in most river studies. However, despite over 100 years of research, recording continuous sediment transport data is challenging due to temporal and spatial variations (Frings and Vollmer 2017; Rickenmann 2017). The following sections describe the current methods for quantifying bedload transport, highlight key studies that use these methods, and review their various advantages and disadvantages.

2.2.1 Channel Form

Channel form changes over time as a result of erosion, transport, and deposition of bed material. The longitudinal profile of a river can be recorded over time and used to identify locations of sediment production and storage (Hicks and Gomez 2003), and assess long-term vertical stability (Simon and Castro 2003). If the upstream sediment supply is enough to satisfy the available stream power then the channel can be said to be vertically stable and the longitudinal profile will show little variation over time (Simon and Castro 2003). However, if upstream sediment supply exceeds the available stream power of the channel then the longitudinal profile will shift until it reaches a more stable state (Lane 1954). This information can be used to locate areas of sediment storage (longitudinal profile is flattening) or sediment production (longitudinal profile is steepening).

Cross sections of a river can identify areas of bank erosion, bar development, and lateral channel migration. These processes can be used to identify areas of sediment production or storage along the channel. Bed level change can also be recorded by performing repeat topographic surveys. This information can further help identify areas of deposition and erosion.

The various types of repeat surveys mentioned above can be useful when looking at long term channel evolution and identifying sources and sinks of sediment in the system. However, these methods provide little insight into how or when the sediment is moving or the size of material that is mobile. In addition, if a channel is in an equilibrium state, these methods may not be able to identify sediment transport because the form of the river may remain static. Documenting the change in channel form is often labour intensive and time consuming. Additionally, several decades of data may be required to assess changes in river form for a particular watershed, making it impractical for graduate student research.

2.2.2 Bulk Sampling

Bulk sampling methods collect all transported sediment in a given area over a given time step. This data can then be integrated over the remainder of the river to obtain a total transport rate. Typically, several

direct bulk samples are taken across a river cross section, with a sample frequency varying between 4 to 10 samples per cross-section depending on the sediment size and size of the river (Frings and Vollmer 2017). Bulk sampling allows for the characterization of all particle sizes in motion as well as an instantaneous estimate of total bed load. However, because most of these methods involve inserting an apparatus into the flow path, several researchers criticize that the presence of the device can alter the flow structure thus skewing the sediment transport mechanisms (Gomez 1991). Additionally, the bed is often disturbed when placing bedload samplers, which can result in an overestimation of the actual sediment transport rates (Bunte et al. 2008; Helley and Smith 1971). Lastly, when using bedload samplers, the sample time is relatively short because of the limited volume each sampler can hold. This short sampling time can greatly impact estimates of bedload transport rates due to the stochastic variability of sediment transport, in particular when dealing with incipient motion of particles (Bunte et al. 2008). The following sub sections describe three of the most common types of bulk sampling devices: pit traps, the Helley-Smith sampler and sediment traps.

2.2.2.1 Pit Traps

Pit Traps are constructed permanent instream bedload measuring devices that consist of an opening where sediment will fall into a pit below (Figure 6). Pit traps are capable of capturing sediment that is either sliding, rolling or making small saltation (Sterling and Church 2002) and have little to no obstruction to the natural flow of the river (Reid, Layman, and Frostick 1980). These traps can be equipped with different devices in order to record continuous bedload transport rates (pressure plates or scales) or systems that can transport the material to a location that can record this type of information (conveyor belts, vortex tubes or sediment pumps) (Gomez 1991; Reid, Layman, and Frostick 1980).

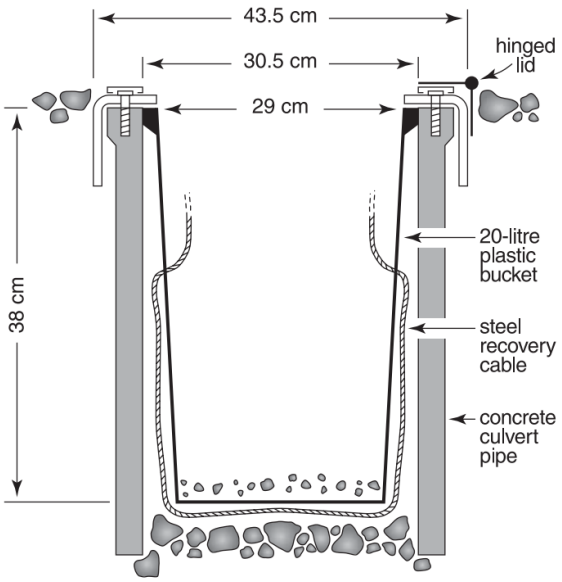

Figure 6 - Example of a Pit Trap. Figure from *Sterling and Church (2002)*

However, pit traps are affected by water circulation inside the trap that can dislodge smaller particles out of the trap (Sterling and Church 2002). Additionally, if the trap is not wide enough (100 to 200 times the diameter of the bed material) then particles could saltate over top of the trap and not be captured (Gomez 1991; Sterling and Church 2002). Lastly, pit traps can be relatively expensive to install, are non-mobile and can only be implemented in shallow and narrow rivers where the bed is easily accessible (Gomez 1991).

2.2.2.2 Helley-Smith Sampler

The Helley-Smith sampler was created for quantifying bedload transport in natural river systems and remains one of the most common tools used. The original sampler has an opening of 76 mm by 76 mm that directs sediment into a mesh sample bag (Figure 7) (Helley and Smith 1971). Due to the relatively small opening, the Helley-Smith sampler is most applicable for use in sand or fine gravel systems where the mean grain size is less than 4 mm (Bunte et al. 2008; Frings and Vollmer 2017). Larger Helley-Smith samplers are available but due their weight, smaller samplers are more commonly used (Bunte et al. 2008).

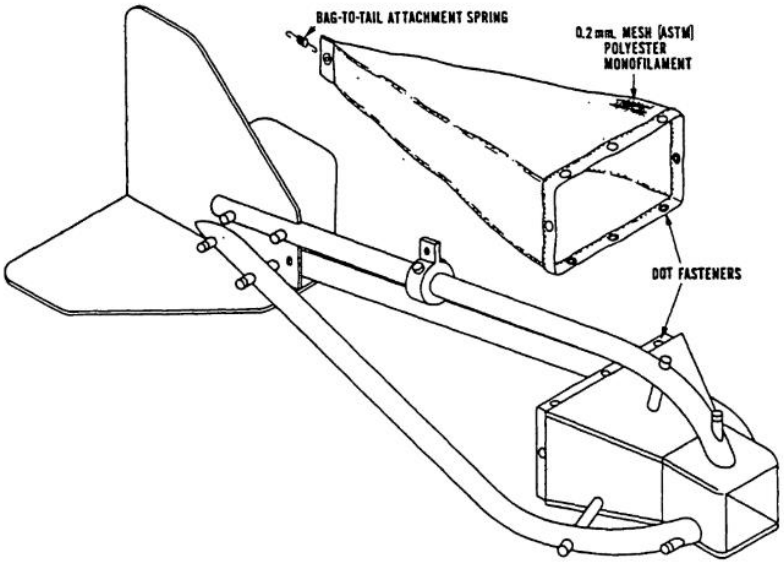

Figure 7 - The original Helley-Smith Sampler design. Figure from *Helley and Smith (1971)*

The main drawback to that Helley-Smith sampler is that they tend to overestimate bedload transport (by up to 50%) because sediment can enter the trap when it is placed on the bed or from the samplers digging into the bed, causing sediment to enter the mesh sampling bag (Helley and Smith 1971). In contrast, it has been reported that Helley-Smith samplers underestimate the bedload transport rate in gravel bed rivers because they are unable to capture the larger sized material that is in sporadic motion (Sterling and Church 2002).

2.2.2.3 Sediment Traps

Originally designed to trap coarse gravel and cobbles, sediment traps have much larger openings and mesh sizes compared to Helley-Smith samplers. It is recommended that the opening is 100 to 200 times the diameter of the median particle size in order to ensure that the majority of larger material is trapped (Gomez 1991). In addition to the larger opening, sediment traps tend to be securely fastened to the bed and have a flap at the opening that supresses the entrance of non-mobile bed material from entering the sampler (Figure 8). Additionally, Bunte et al. (2008) found that in mountain streams sediment traps allowed debris, such as twigs and leaves, to escape through the larger mesh size, as opposed to the Helley-Smith sampler, which retained this material.

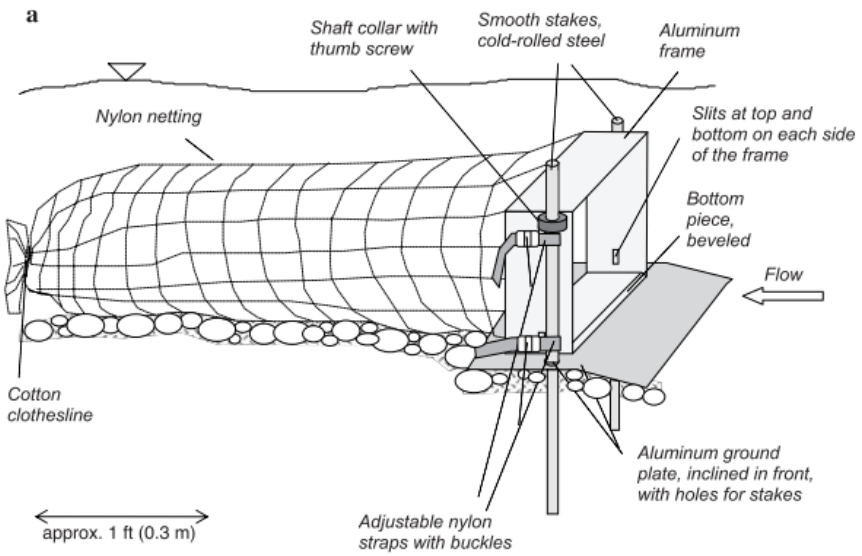

Figure 8 - Example of a Sediment Trap. Figure from *Bunte et al.(2008)*

2.2.3 Indirect Sampling

Indirect sampling methods measure a surrogate parameter that can be related to bedload transport. These parameters vary depending on the size of sediment and scale of study area. One main advantage of using indirect methods compared to direct methods is that they tend to be non-intrusive, but they can require intensive calibration depending on the chosen surrogate parameter (Koshiba et al. 2018; Rickenmann 2017; Wyss et al. 2016). This section describes some of the methods used for indirectly measuring bedload transport.

2.2.3.1 Passive Acoustic Measuring Devices

Passive acoustic measuring devices use sound waves or vibrations caused by particle movement to determine bedload transport parameters including total bedload intensities/mass (Beylich and Laute 2014; Rickenmann 2017; Rickenmann et al. 2014), bedload grain size distributions (Rickenmann 2017; Wyss et al. 2016), and the timeline of bedload transport (Beylich and Laute 2014). In order to obtain accurate readings, calibration of the equipment against bedload transport field data or flume data is required (Rickenmann 2017). Therefore, this indirect method typically requires some direct sampling to be done at the study site for calibration.

The two most common passive acoustic measuring devices are hydrophones and impact plates (Figure 9). Hydrophones listen for sound created by the collision of moving particles, while impact plates measure the vibration caused by mobile particles impacting a plate on the channel bed (Rickenmann 2017).

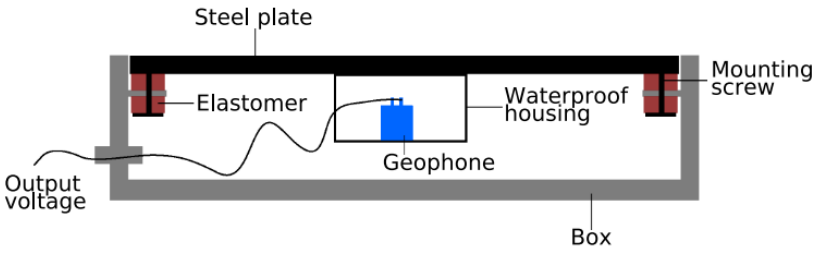

Figure 9 - Example design of a Swiss Plate Geophone. Figure from *Wyss et al. (2016)*

In addition to providing continuous data on bedload transport, impact plates do not alter the natural flow patterns because they can be placed flush with the native bed material (Beylich and Laute 2014; Rickenmann 2017). However, they do require installation in an area where the bed is stationary in order to ensure the apparatus remains immobile (Beylich and Laute 2014). Impact plates are installed in rivers as a research tool but several studies have reported noise interference from flow turbulence (Rickenmann et al. 2014).

2.2.3.2 Acoustic Doppler Profilers (ADP)

Acoustic doppler Profilers (ADP) are commonly used to determine flow velocities and bed location by sending a series of acoustic pulses at different frequencies. If the ADP is placed on a moving object, such as a boat, it can determine the boat's velocity using the shift in the frequency of the return signal. If the river's bed is moving as well, then the shift in signal would be a combination of the boat velocity and the bed material velocity (Rennie, Millar, and Church 2002). Rennie et al. (2002) were the first to test this theory in the field by mounting an ADP on a boat and recording the shift in frequency relative to the boat velocity which gave an estimated bedload velocity. These results were then compared to data from a direct sampling method and were found to be highly correlated, meaning calibration curves can be created using this technology (Rennie et al., 2002).

2.2.4 Sediment Tracking

Since sediment transport is a function of the movement of individual grains, researchers have also quantified bedload transport by measuring the movement of individual particles of varying sizes. Einstein (1937) was the first to visually track particles in a flume and observed that individual particles move in a series of steps and rests that together make up their total travel distance (Einstein 1937). This stochastic movement observed by Einstein has further been documented in lab and field studies, which has created a sub section of sediment transport research that revolves around sediment tracking. Field specific sediment tracking involved some form of tagging individual particles of varying sizes and recording their position after a given amount of time, either annually or after large flow events. The total travel distance and burial depth of the particles can then be related back to total bedload transport. There are several different methods of tagging individual stones that includes, but is not limited to, exotic particle tracking, painted stone tracking, magnetic stone tracking, and RFID stone tracking.

2.2.4.1 Exotic Material

Exotic material is one of the simplest methods of particle tracing (Hassan and Ergensinger 2003). The method involves placing foreign material that is visually identifiable into the stream and recording the foreign particles movement after high flow events or a specific time interval. Particles can be marked with unique identification numbers or left unmarked. Mosley (1978) introduced limestone (which is golden compared to the grey native material) into the Tamaki River, New Zealand to characterize the mobilization of bed material after high flow events. This technique introduced particles of all sizes, however only particles greater than 8 mm were tracked. Despite this being a low cost and easily implementable alternative (Hassan and Ergensinger 2003), a recovery rate of only 5% was reported (Mosley, 1978).

More recently, Houbrechts et al. (2011) tracked iron slag deposits on riffles along the longitudinal profile of a series of rivers in south-eastern Belgium. Various historic iron works (active from 1542 to 1850) injected iron slags into the watershed from various furnaces or refineries, which are easily identifiable

compared to the other naturally occurring sediment. The ten largest pieces of slag deposited on each riffle were documented and used to infer the maximum effective competence of the river (Houbrechts et al. 2011). Additionally, fronts of iron slag were identified and estimated travel rates between 2 to 4 km/century were reported (Houbrechts et al. 2011). The authors developed an innovative approach to sediment tracking using tracers that enabled researches to shed light on river processes dating back centuries.

2.2.4.2 Painted Stones

Similarly, to tracking exotic material, painted stone tracers are placed in the study area and repeat visual inspections are conducted after an event or a specific time interval. This method involves sampling sediment from the study area, painting them a bright colour, and assigning each a unique identification number. Once a flood occurs stones are located, the identification number and location will be recorded. If the study is looking at long term movement, the stones will be placed back where they found until another event occurs. This method is also relatively cheap but similarly to exotic material tracers experiences low recovery rates, is limited to surface use, and the paint tends to wear off after a couple events (Hassan and Ergensinger 2003).

Leopold et al. (1966) was one of the first studies to deploy a large number of painted stone tracers. This study tracked particles to assess whether clusters of particles are less mobile than particles that are separated. To accomplish this, over 14,000 observations of particles spaced at different intervals were made (Leopold, Emmett, and Myrick 1966). Recovery rates ranged from 90% in smaller floods, to only 2% in an "exceptionally large flood", leading to the conclusion that loss rates of 10-30% in small flows and up to 30-50% in large flows can be expected when using painted stone tracers (Leopold, Emmett, and Myrick 1966). Paint integrity and tracer identification after transport were reported as key challenges (Leopold, Emmett, and Myrick 1966). Even if all the tracers remained identifiable, several were unrecoverable due to burial, entrainment in bushy areas, and movement outside of the study reach (Leopold, Emmett, and

Myrick 1966). Despite relatively low recovery rates, results indicated that larger flows are required to move particles located closer to one another (Leopold, Emmett, and Myrick 1966).

Laronne and Carson (1976) found even lower recovery rates of 5% (0.5% for smaller material and up to 100% for larger material). In this study, tracers were placed directly on the surface (where they are visible) and replaced on the surface after each event. Results demonstrated how such methodologies have an inherent biased towards higher travel distances because the particles are more likely to move than their in-situ counterparts due to higher exposure to the flow (Church and Hassan 1992; Laronne and Carson 1976).

2.2.4.3 Magnetic Stones

Magnetic tracers are either naturally magnetic stones, artificially magnetic stones or stones with magnets inserted into them (Hassan and Ergensinger 2003). When these traces pass through a magnetic field they generate an electric signal that identifies their presence and can be detected by a recorder (Figure 10) (Ergenzinger and Conrady 1982).

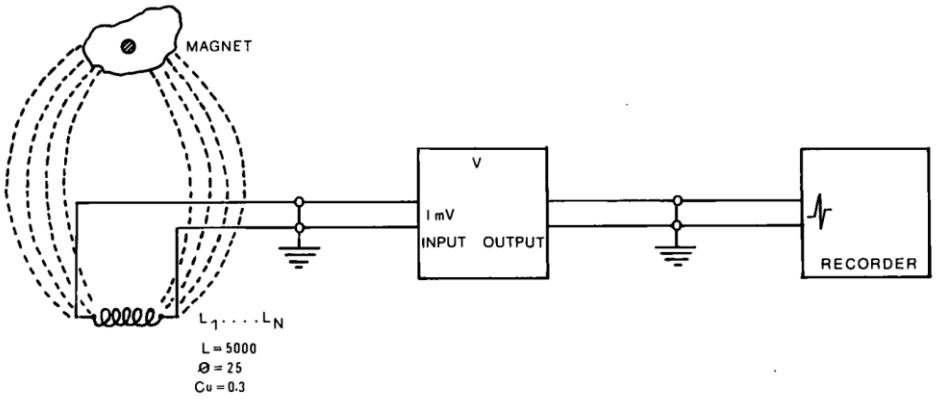

Figure 10 - Original magnetic tracer setup. Figure from *Ergenzinger and Conrady (1982)*

The main advantages to using magnetic tracers is that they can be detected below the surface (compared to the previously mentioned technologies that can only be tested at the surface), and that a wider range of particle sizes can be tagged. However, this method is costly compared to others, and the creation of

the stones is relatively labour intensive. Additionally, detection of tracers may be shielded if the site has naturally occurring magnetic properties (Hassan and Ergensinger 2003).

Since these particles can be tracked below the ground surface, burial depth of the particles can be determined. Hassan (1990) looked at the influence of burial depth on sediment transport and the morphology of the Nahal Hebron and Nahal Og, Israel using magnetic particles. Recovery rates between 55% to 93% were achieved, of which 33% to 87% of tracers were buried (Hassan 1990). In order to determine the burial depth, the bed material on top of the tracer needs to be removed. The tracers can then be left in the bed material or placed back on the surface. However, disturbing the bed can alter the sediment transport proprieties of the surrounding bed. Additionally, tracking and locating buried sediment can be extremely time consuming. Schmidt and Ergensinger (1992) used magnetic tracers to determine the effect of particle size and shape on travel distance, movement probability, and burial depth. Due to the long time it took to complete a recovery, large amounts of data was lost in between closely-spaced high flow events (Schmidt and Ergensinger 1992).

2.2.4.4 Passive radio frequency identification transponders (RFID)

Radio Frequency Identification (RFID) technology has been used for sediment transport research applications. Passive Integrated Transponders (PIT tags) are passive RFID tags that have no internal power source. As such, PIT tags have been used to track animals for many decades and have more recently been used for tracking sediment in rivers, beaches and other fluvial environments. PIT tags are either placed within a stone by drilling a hole and sealing it with an adhesive, or by fabricating an artificial stone around the PIT tag. The main advantages of using RFID compared to other tracking strategies is the low cost, absence of internal battery, and the unique identification number (Allan, Hart, and Tranquili 2006; Bradley and Tucker 2012; Camenen et al. 2010; Cassel, Dépret, and Piégay 2017; Cassel, Piégay, and Lavé 2016; Chapuis et al. 2014, 2015; Ford 2014; Liébault et al. 2012; Macvicar et al. 2015; C. B. Phillips and Jerolmack 2014). Additionally, unlike their magnetic counterparts, RFID tracers can be identified below the ground

surface without disturbing the bed material (Schneider et al. 2014). However, several studies have reported low recovery rates due to tracer burial and the limited detection zones of the tracers (Chapuis et al. 2014).

The size of the detection zone increases with the size of the PIT tag. The orientation of an PIT tag can also affect the size of the detection field by up to 37% (Arnaud et al. 2015). The most effective position relative to the antenna for an PIT tag to maximize the probability of detection is vertical (Chapuis et al. 2014) due to the variability of detection field shape based on orientation (Figure 11). However, since tracer stones move as a result of rolling or hopping, it is impossible to ensure the PIT tag will remain upright in most bedload tracking applications.

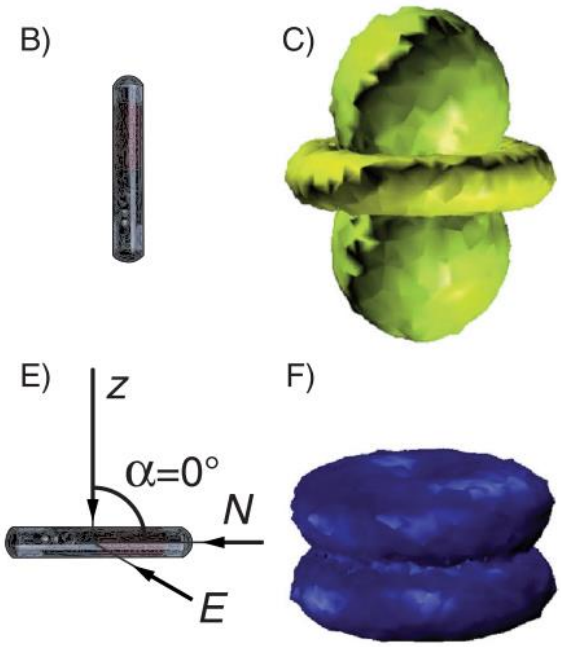

Figure 11 - Detection field of an PIT tag. Figure From *Chapuis et al. (2014)*

PIT tags have also been used to determine the 3D location of underground assets (Dziadak et al. 2009). Dziadak et al. (2009) proposed a procedure to determine the depth of buried pipes. If the tag is vertical, the burial depth can be determined by raising an antenna above the location of the tag until it can no longer detect the tag (Dziadak et al. 2009). The distance between the ground and the antenna (*Z*) can be

subtracted from the known height of the detection zone of the vertical tag (*H*) to obtain the burial depth (*D*) (Figure 12). However, for this methodology to be applicable for tracking sediment, there would need to be way to ensure the orientation of the PIT tag remains vertical at all times. Additionally, depending on the buried material and how far the tag is buried, the signal strength can be decreased by up to 20% (Dziadak et al. 2009).

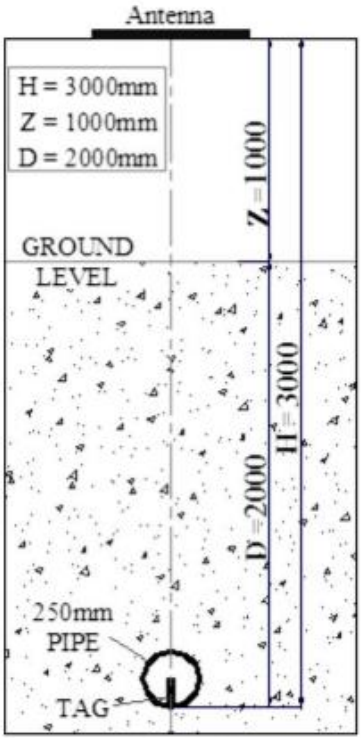

Figure 12 - Procedure for determining burial depth of pipe. Figure from *Dziadak et al. (2009)*

Papangelakis et al. (2019) developed a self-righting apparatus (a 'wobblestone') that holds a PIT tag and can be placed inside a fabricated stone. Preliminary lab tests using a 12mm tag indicate the PIT tags remained vertical regardless of the stone orientation, and that burial depth could be predicted to +/-1 cm using the height above the bed at which the tag was first detected (Papangelakis et al. 2019). The burial depth can be used to assess the active depth of transport which can be used to calculate total bedload transport. However, these stones have not yet been produced in large quantities or tested in a field setting, and a field method and/or apparatus for determining burial depth remains to be created.

2.3 Longitudinal Profiles

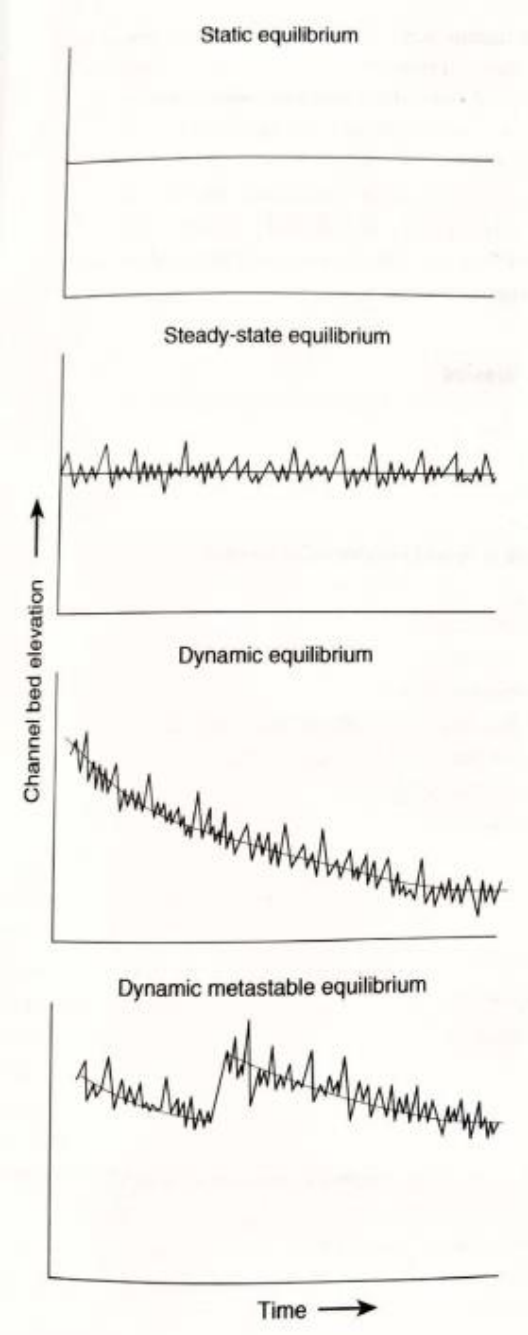

Figure 13 - Comparison of different Types of equilibrium. Figure from *Charlton (2008)*

The longitudinal profile of a river is a plot of bed elevation versus distance along the river and is typically described as a concave-upward curve (decreasing slope in the downstream direction) (Dade and Friend 1998; Gasparini, Tucker, and Bras 2004; Parker 1991; Snow and Slingerland 1987). These profiles have been described quantitatively using several mathematical models including: linear (Ohmori 1991), quadratic (Rice and Church 2001), exponential (Ohmori 1991; Shulits 1941; Snow and Slingerland 1987; Yatsu 1955), logarithmic (Snow and Slingerland 1987), and power function (Ohmori 1991; Shepherd 1985; Snow and Slingerland 1987). The main factors effecting the shape of river longitudinal profiles are sediment size, sediment load, flow rate, and tributary inputs (Rice and Church 2001).

2.3.1 Temporal and Spatial Scale

Both temporal and spatial scale play an important role when studying any type of landform evolution, especially rivers. Spatial scale can encompass a whole watershed or can focus on individual grains, while temporal scale can range from a few seconds to hundreds of thousands of years. At the watershed scale, cumulative effects of long-term processes can be examined in contrast to smaller scales where interactions between processes, form and individual variables can be identified.

Additionally, depending on the temporal scale of study, different equilibrium conditions can be identified (Figure 13) (Charlton 2008).

For example, static equilibrium can be observed over short time periods such as short-term field monitoring programs, while steady state equilibrium might be observed in longer term field programs lasting decades. If even a larger temporal scale is used, dynamic equilibrium patterns can be observed as a river gradually erodes over the time span of thousands of years. Lastly, dynamic equilibrium can be altered by drastic short-term changes such as localized uplift or fault line movement, this can cause a dynamic metastable equilibrium (Charlton 2008).

2.3.2 The Graded River

One of the most accepted descriptions of equilibrium in rivers was proposed by Mackin (1948) and is known as the graded river. A graded river will continually try to adjust its longitudinal profile (the slope of the channel) in order to reach a balanced state where the velocity is equal to the velocity required to transport the supplied material, under prevailing channel conditions and available discharge (Mackin 1948). These adjustments typically happen on a reach scale (segment of a river with uniform characteristics including but not limited to: geometry, slope, and geology) and on the temporal magnitude of years to decades. When comparing this equilibrium state to Figure 13, a graded river can be classified as steady-state equilibrium that occurs on a reach basis, while the watershed scale is most likely in a dynamic equilibrium.

This concept was further developed by Lane (1954) who related physical channel characteristics to the sediment transport parameters:

$$Q_s D \propto Q_w S \tag{7}$$

where Q_s, D, Q_s and S are the sediment discharge, particle diameter or size of the sediment, water discharge and the slope of the stream, respectively. This equilibrium equation suggests that a stream will

remain in an equilibrium state if these four parameters are balanced. If one of these parameters is modified the other three parameters will shift until a new equilibrium is reached. However, this relationship does not indicate which parameters will change or how long it will take to reach a new equilibrium. The Lane equilibrium concept has since been visualized as a tipping scale (Figure 14).

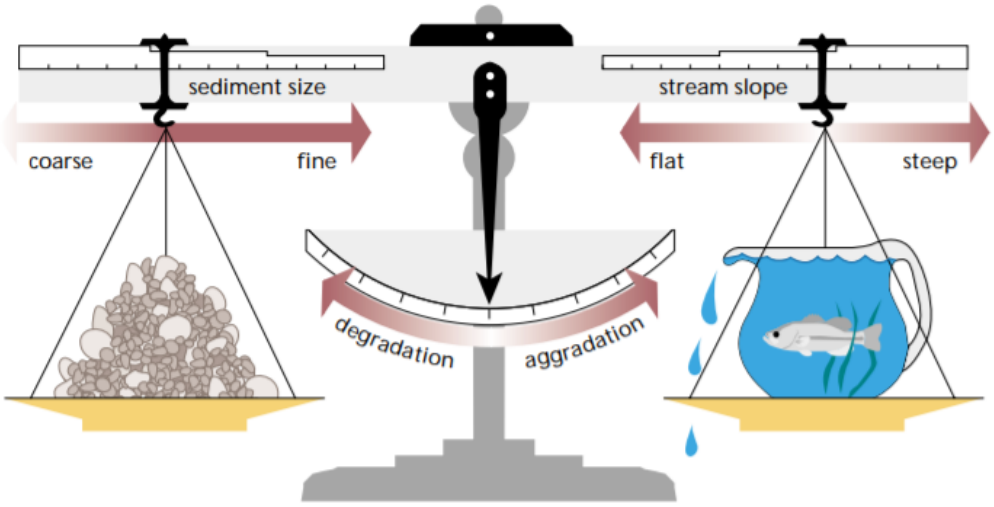

Figure 14 - Lane's Balance. Figure from *FISRWG (1998)*

Sediment supply and size is a function of upstream geologic features and erosion processes as opposed to discharge, which is affected by watershed properties and climate conditions. At a reach scale and over a relatively short temporal scale (tens to hundreds of years), the slope of the river is typically the parameter that will be altered to absorb upstream or watershed changes (Hoover 1948; Schumm and Lichty 1965; Yatsu 1955). As the bed slope declines, the river capacity to transport larger material decreases as a result of decreasing flows, shear stress and stream power (Dade and Friend 1998; Smith and Ferguson 1996), typically resulting in downstream fining trends (Rice and Church 1998).

2.3.3 Downstream Fining

Observations show that, in natural rivers, the average size of bed material decreases from upstream to downstream as a result of two main processes: abrasion and selective sorting of particles (Dade and Friend 1998; Knighton 1982; Parker 1991; Rice and Church 1998). Abrasion is a form of mechanical weathering that causes particles to break up over time as they are transported downstream. In contrast, selective

sorting is a combination of several processes that can cause smaller particles to move farther during transport (Rice and Church 1998).

For example, most boulder-sized material (>248 mm) tends to remain in upstream sections and only moves during exceptionally high flow conditions (Knighton, 1982). On the other hand, finer sediment such as silt and clay (<0.06 mm) tend move as suspended sediment and only deposits in slow moving environments, such as pools, or in flatter sections downstream. Medium-sized material such as cobbles (64 mm – 248 mm) can move along the bottom of the channel during high flow events. If this medium-sized sediment is relatively soft (limestone, sandstone) the particles can be broken up into finer pieces that will move farther downstream during smaller flow events (Parker 1991).

As the slope of a channel decreases downstream, stream flow increases, stream power increases then decreases and a transition of bed material from gravel to sand is commonly visible (Figure 15) (Church 2002). This decrease in bed material size results in a decrease in bed roughness, which can cause an increase in bed velocity, bed erosion, and sediment transport (Smith and Ferguson 1996).

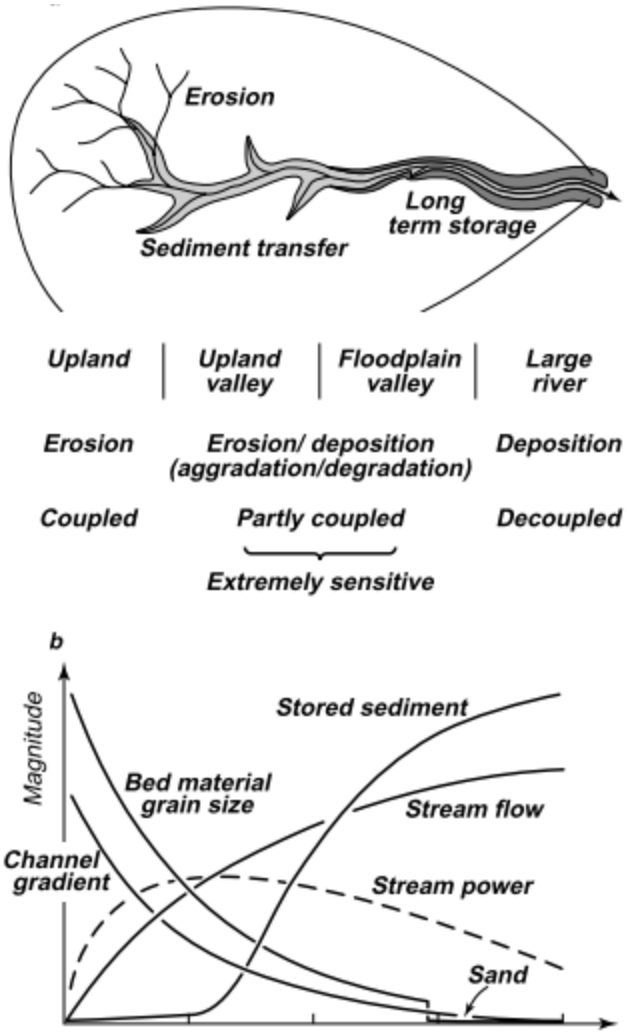

Figure 15 - Sediment composition decreasing down stream. Figure from *Church (2002)*

The process of downstream finding tends to occur over several kilometres; but researches have noted abrupt downstream fining trends that occur over much shorter distances (Ferguson 2003; Parker 1991). Downstream fining over shorter distances can be related to different sediment inputs along the longitudinal profile. If material that does not match the bed material enters the river from a tributary, bed erosion, or bank failure, the introduced material can have significant impacts on the local sediment characteristics (Dade and Friend 1998; Knighton 1999).

Larger material that is introduced to the stream can get trapped if the stream does not have enough capacity to transport it further downstream (Dade and Friend 1998). This can cause an increase in bed roughness, a decrease in velocity, and local aggradation of the bed. In addition, the larger material will act as an armouring layer, which will further inhibit the stream from transporting material in this section. Knighton (1999) examined a stream where mining practices introduced material much smaller than the native bed material. The influx of fine sediment caused a sharp change in the bed material from gravel to sand over a stretch of less than 500 m (Knighton 1999).

2.4 River Evolution Models

Over time, rivers transport sediment as they convey flow downstream, which gives them the potential to form and erode floodplains and other sediment deposits. This section provides a brief overview of the commonly used evolution models for both urbanized and un-urbanized watersheds.

2.4.1 Urbanized River Evolution Models

Urbanization is defined by the United Nations as "the process by which a large number of people become permanently concentrated in relatively small areas, forming cities" (United Nations 1997). When an area becomes urbanized the percent of impervious surfaces tends to increase (Allmendinger et al. 2007; Chin 2006; Paul and Meyer 2001; Walsh et al. 2005).

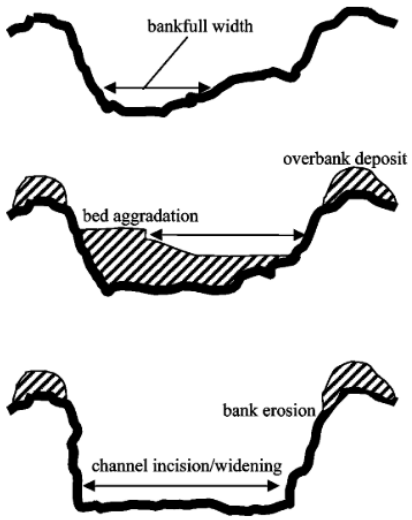

Figure 16 - 2 Phase urbanized river evolution model. Figure from Paul and Meyer (2001)

Paul and Meyer (2001) conducted a review of several studies that examined the impact of urbanization on the ecology of river systems. They suggested a two-stage model that shows how a typical river will evolve during urbanization (Figure 16). The first phase occurs during construction and is referred to as the aggradation stage. The aggradation stage is characterized by bed aggradation and a decrease in hydraulic capacity, driven by the increase in sediment yield as a result of construction activities. Since the system has a lower hydraulic capacity, flooding will occur, causing further aggradation on the floodplain (Paul and Meyer 2001).

The next phase is known as the erosion phase and is mainly driven by the changes in hydrology as a result of the increase of impervious surfaces in the watershed. The increase in runoff and decrease in infiltration causes the shape of flow hydrographs to become flashier, characterized by shorter events with higher magnitude peak flows. These changes cause an increase in flow velocities and erosion which leads to wider and deeper rivers (Paul and Meyer 2001). In addition, a decrease in infiltration can reduce baseflows

and alter the water temperature. Lastly, the erosion phase is also characterized by a decrease in sediment supply and size, which can cause the river to decrease in shape complexity and become straighter (Chin 2006; Walsh et al. 2005).

Chin (2006) further developed this model by adding two additional phases to create a five-phase model (A through E). Phase A represents a lag time between when construction starts, and when morphological change is seen. Phase B is analogous to the construction phase in the Paul and Meyer (2001) model where channel aggregation occurs due to increased sediment yield. Phase C represents the shift from aggradation to erosion where the sediment that built up in Phase B is washed out due to the change in runoff volumes. Phase D is where erosion continues and channel enlargement (both width and depth) occurs. Lastly, Phase E represents a new stable equilibrium point that the river could reach if construction and urbanization fully stops and the river has sufficient time to stabilize (Chin 2006).

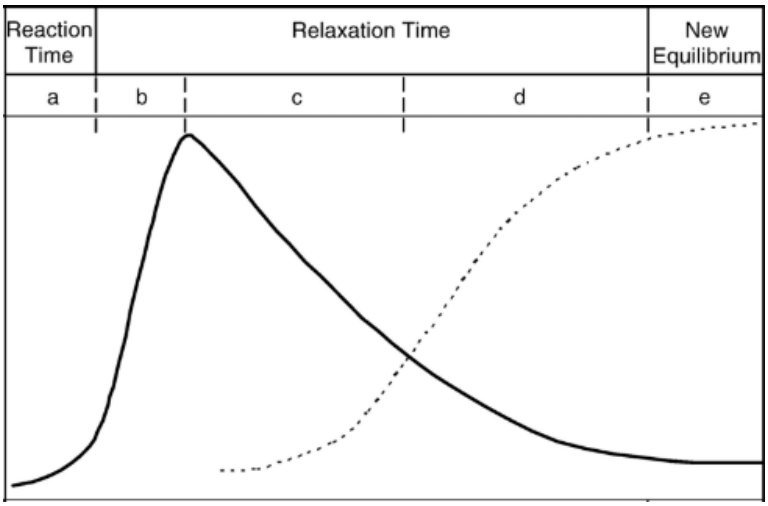

Figure 17 – Changes to sediment yield (solid line) and runoff (dashed line) over the course of the channel's evolution. Figure from Chin (2006)

2.4.2 Semi-Alluvial Rivers

Semi-alluvial rivers contain both sections of mobile sediment and exposed bedrock. Mobile sediment can be introduced into the stream from upstream sources, tributaries, or through bedrock erosion. Semi-alluvial rivers in Southern Ontario move through a diverse mix of glacial landforms left behind by the melt

of the Laurentide Ice Sheet in the Quaternary Period (R. Phillips and Desloges 2015b, 2015a). The bed material is comprised of a large heterogeneous deposits of cohesive glacial till that contains material ranging from clay to boulders (Pike, Gaskin, and Ashmore 2017). When exposed, glacial till behaves like sheets of soft bedrock and can restrict the vertical and horizontal adjustment of a river (Gallagher, Balme, and Clifford 2017; Thayer and Ashmore 2016).

The main difference between the typical graded river and semi-alluvial glacial till (SAGT) rivers found in southern Ontario is that their headwaters are located on flat plains that do not produce as much sediment supply as the typical mountainous headwater depicted in Figure 18 (Phillips and Desloges 2015b). Alluvial bed material in SAGT systems are heavily dependent on the sediment availability and erosion of the glacial bed material (Gallagher et al. 2017; Phillips and Desloges 2015b; Rice and Church 1998; Thayer et al. 2016). Exposed till acts as a lateral sediment source that creates discontinuities in downstream slope and sediment trends commonly associated with graded rivers (Phillips and Desloges 2015b; Rice and Church 1998; Thayer et al. 2016). As the exposed glacial till erodes, the finer material (clays and silts) gets transported downstream as suspended sediment, leaving the coarser sediments behind (Thayer, Phillips, and Desloges 2016). The coarser sediment introduced into the river from the erosion of the glacial till typically remains immobile, which inhibits further erosion of the material below (Gran et al. 2013). Areas of local downstream fining are commonly referred to as sediment links. The upstream potion of these links is characterized by steep sections with relatively coarse material. Towards the downstream end of the links, the slope will flatten out and the bed is typically composed of finer gravel or sand (Figure 18 and Figure 19) (Phillips & Desloges, 2015b; Rice & Church, 1998; Thayer et al., 2016).

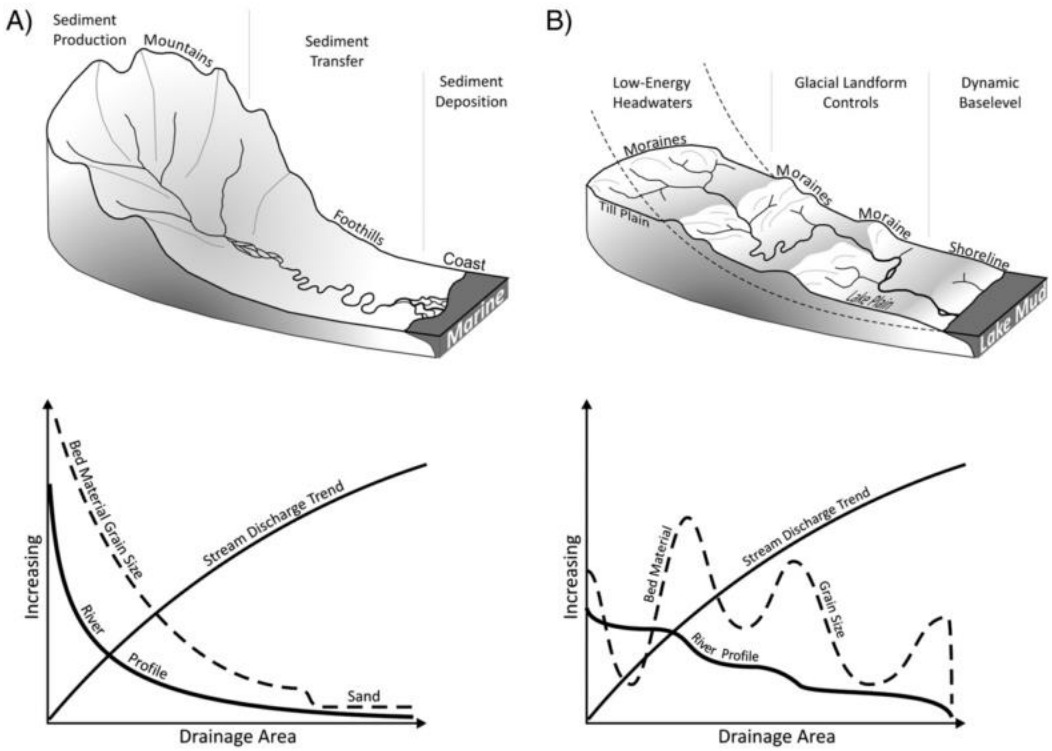

Figure 18 – Comparison of downstream trends in a graded river and glacially influenced rivers located in southern Ontario. Figure from: *Phillips and Desloges (2015b)*.

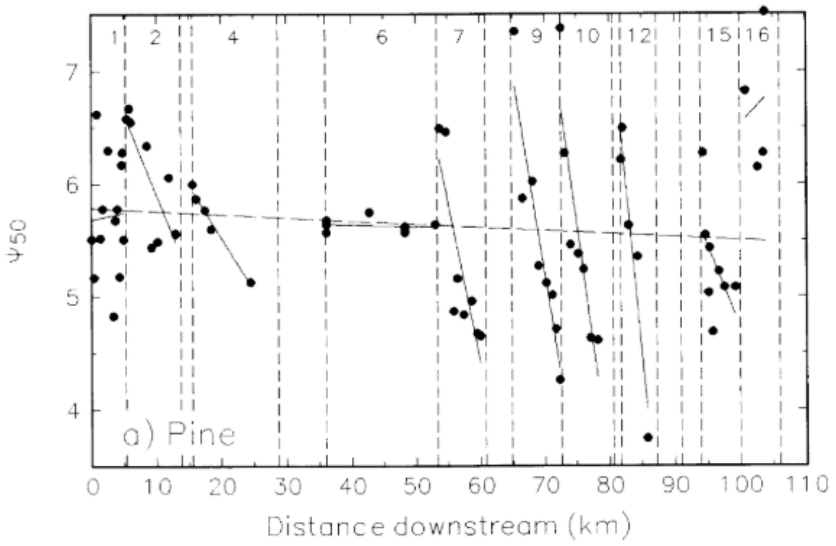

Figure 19 - Exampled of sediment links fining trends. Figure from *Rice and Church (1998)*

Bevan et al. (2018) proposed a channel evolution model for an urbanized SAGT river in Toronto, Ontario. Five stages were identified: pre-urbanization, widening with meander expansion, avulsion, incision and bank retreat (Figure 20). The first pre-urban stage is characterized by coarse riffles with little sediment mobility due to the oversized material introduced into the channel, this larger material provides resilience to bed erosion but encourages bank erosion and meander extension. As a result, avulsion of the meanders (cutting off of the bend) can occur resulting in wider and straighter reach that produces enough stream power to transport the larger material that is protecting the bed. From here, the bed will begin to erode resulting in a deeper channel (Bevan et al. 2018).

An opportunity exists to further investigate the evolution of sediment links on SAGT rivers. These steep high stress areas could be prone to increase erosion as a result of urbanization, however more needs to be done to confirm this theory. A baseline condition for how these systems behave before urbanization is necessary in order to understand, predict, and prevent impacts of future urbanization.

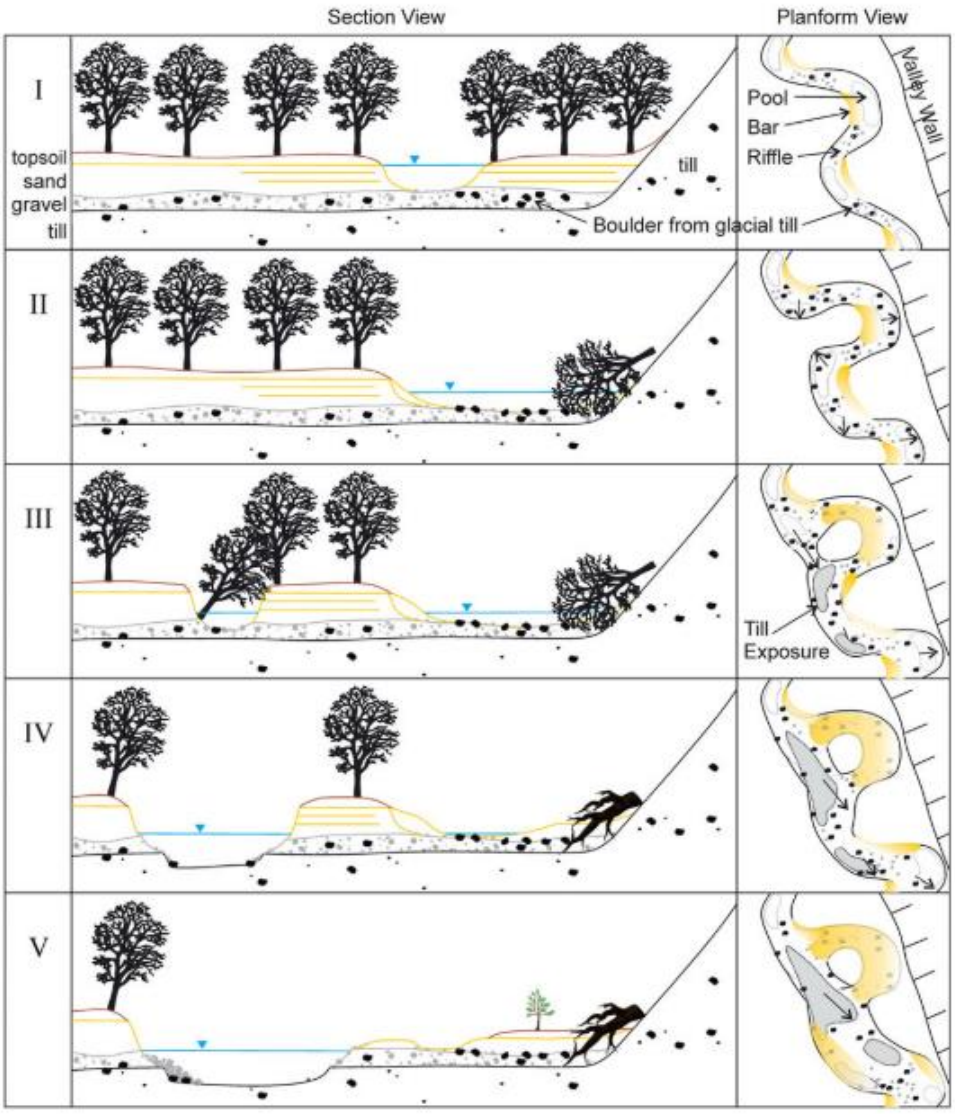

Figure 20 – Proposed evolution model for a semi-alluvial glacial till river in southern Ontario. Figure from *Papangelakis et al. (2019)*

2.5 Summary of Research Gap

Two research gaps have been identified in the previous sections. The first relates to the methodological deficiency in measuring sediment transport and the burial depth of tracer stones. This gap will be addressed with the first objective of this thesis which is to demonstrate the effectiveness of a new high-precision bedload transport tracking technique developed by Papangelakis et al. (2019) called a 'wobblestone'. The second research gap that will be addressed in this thesis relates to the characterization

of a semi-alluvial glacial till river in southern Ontario prior to urbanization. This will be done by characterizing the western branch of Ganatsekiagon Creek in Pickering, Ontario.

Chapter 3 – Field Tests of Wobblestone Tracers for Sediment Transport Research

'Wobblestones' are a type of sediment tracer developed by Papangelakis et al. (2019) that maintains an upright position of the PIT tag during transport, which was shown in laboratory tests to improve the precision of the estimate of the location of the tracer and allowed the burial depth to be determined. These tracers are comprised of two parts, the RFID insert and the fabricated shell. The RFID insert is made up of a weighted inner ball that holds a 12mm PIT tag, a lubricant and an outer ball (Figure 21). The lubricant allows the inner ball to freely rotate inside the outer ball. The fabricated shell mimics the density and shape of a natural stone. The following sections describe the tracer fabrication process, prototype testing procedure and results, a device developed to help estimate tracer burial depth, and the tracer test results following a 1-year deployment with significant movement of bed material in Ganatsekiagon Creek.

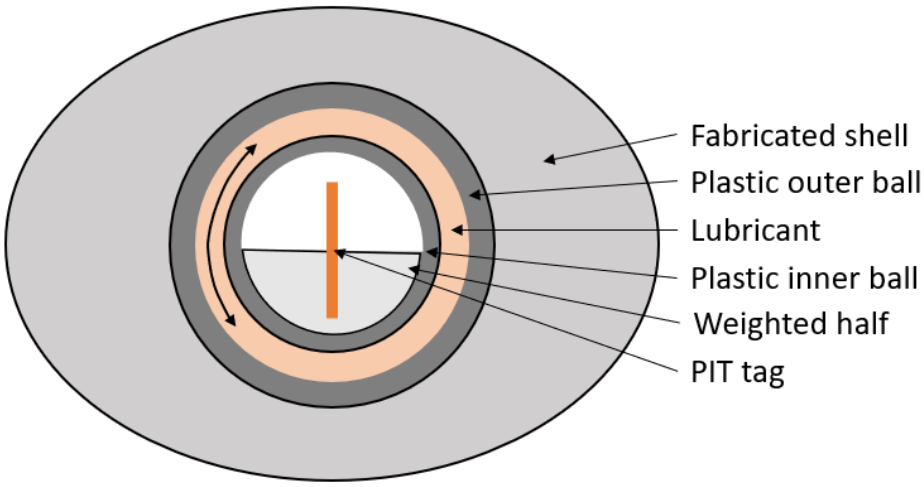

Figure 21 – Wobblestone conceptual model, modified from Papangelakis et al. (2019)

3.1 Tracer Fabrication

Stone molds were made following the procedure outlined in Cassel et al. (2016). The molds were made of three different stone sizes (small, medium and large) from a Mold Star® 15 slow platinum silicone rubber (see Table 3 for sizes, Figure 22a). The liquid silicone was poured over the real stones and left to cure for

approximately 24 hours. The cured silicone was then cut, and the real stone was removed to create a negative impression of the stone in two halves.

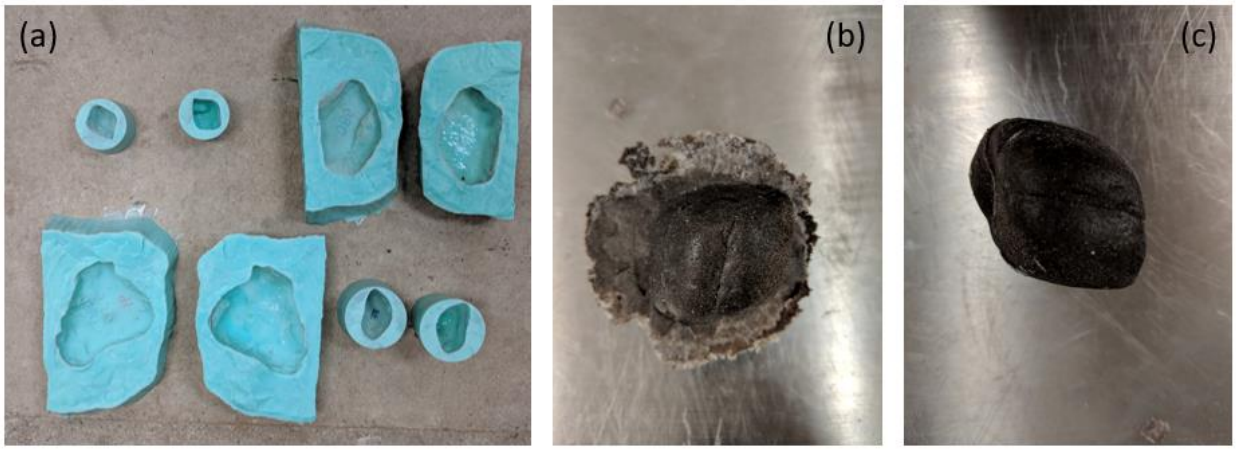

Figure 22 – (a) Fabricated shell mold (b) Completed tracer with excess material (c) Tracer without excess material

RFID inserts were fabricated as per the procedure outlined in Papangelakis et al. (2019). The plastic inner and outer balls were fabricated using a high-density polyethylene that was injected into a custom milled aluminum mold. The aluminum mold and the four RFID insert parts (2 inner halves and 2 outer halves) can be seen in Figure 23.

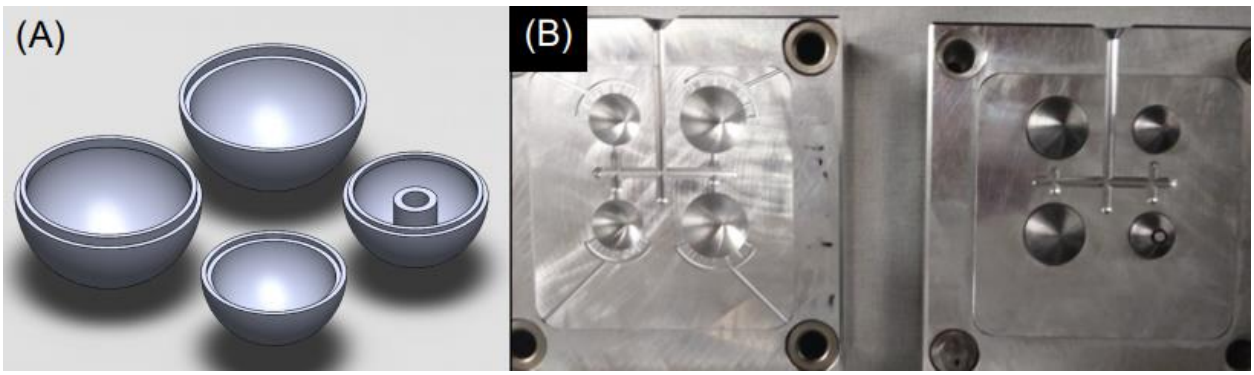

Figure 23 - (a) Design drawing of plastic injection Part (b) Injection mold (Papangelakis et al., 2019)

The bottom half of the inner ball was weighted with a 1:2 mixture of high-density resin and fine aluminum oxide (Al_2O_3) (240 grit). A 12.0 mm x 2.12 mm HDX ISO 11784/11785 PIT tag was then placed inside the

bottom half of the inner ball so that the copper coil was pointing upwards, which is the orientation that maximizes the detection range (Chapuis et al. 2014). The two halves of the inner ball were secured together using a waterproof epoxy. After the 24h drying period, each inner ball was manually inspected to ensure that the outside was free of epoxy residue and that the two halves were secured. The outer ball was filled with 0.3 mL of a glycol solution (70% glycerine and 30% water), the inner ball was placed inside the outer ball, and the outer ball was sealed with an epoxy sealant. Glycol was selected as the ideal lubricant because it is non-toxic and has a low freezing point of -38°C when mixed in a solution of 70% glycerine and 30% water (Papangelakis et al. 2019). After the 24h drying period, all RFID inserts were visually inspected to ensure the inner ball freely rotated and that the seals were free from leaks.

The fabricated shell was created around the RFID insert following the basic procedure outlined in Cassel et al. (2016). A putty like mixture of high-density polyurethane plastic resin (Smooth-Cast® 380 manufactured by Smooth-On), aluminum oxide (Al_2O_3) and/or gravel was placed inside each half of the mold. The RFID insert was placed in the middle of the bottom half of each mold. The two halves of the mold were placed together, and a weight was placed on top of the molds to ensure that the two halves of each shell stuck together. After one hour, the completed wobblestone was removed from the mold and any excess material was removed from the outside edge of the stone (Figure 22b and Figure 22c). The final stone was allowed to dry for a minimum of 24 hours to ensure that the resin had fully set.

3.2 Prototype Testing and Results

Particle tracer stones in three particle size classes were made and tested for density and durability using several combinations of high-density resin, fine and coarse corundum (Al_2O_3) power, and natural gravel for filler. Cassel et al. (2016) used a 9:41 ratio of resin to fine Al_2O_3, while Papangelakis et al. (2019) used a ratio of 1:2, but for the current study: sand, gravel and coarse Al_2O_3 were rested as part of the mixture to reduce costs as a replacement for fine Al_2O_3. The densities of these material and their cost per unit

weight are presented in Table 1. Material ratios, final densities and final cost for each tracer are presented in Table 2 for comparison.

Table 1 - Material specifications

Material	Density	Cost
Aluminum Oxide (Al_2O_3) – Fine (240 Grit)	1.93 g/cm^3	15.40 CAD / kg
Aluminum Oxide (Al_2O_3) – Coarse (80 Grit)	2.01 g/ cm^3	5.06 CAD / kg
All Purpose Sand	1.27 g/ cm^3	0.29 CAD / kg
All Purpose Gravel	1.25 g/ cm^3	0.26 CAD / kg
High Density Resin	1.78 g/ cm^3	4.03 CAD / kg

Table 2 – Prototype stones, the highlighted rows indicate the chosen material ratios

Sample Number	Percent by Volume					Density (g/mL)	Cost (CAD/kg)
	Sand	Al_2O_3 - Fine	Al_2O_3 - Coarse	Gravel	Resin		
1	-	67%	-	-	33%	2.27	11.81
2	-	57%	-	14%	29%	2.49	10.66
3	-	50%	-	25%	25%	2.33	9.72
4	-	43%	-	29%	29%	2.39	8.79
5	-	38%	-	38%	25%	2.44	7.98
6	67%	-	-	-	33%	1.82	1.83
7	57%	-	-	14%	29%	2.15	1.63
8	50%	-	-	25%	25%	2.08	1.48
9	43%	-	-	29%	29%	2.09	1.63
10	38%	-	-	38%	25%	2.18	1.48
11	-	-	67%	-	33%	2.68	4.74
12	-	-	50%	25%	25%	2.48	3.95
13	-	-	43%	29%	29%	2.53	3.76

The target density of the tracers varies between 2.54 and 2.66 g/cm^3 based on densities measured in the field. To compensate for the void in the middle of the stone where the RFID insert is located, a higher density material than the target density is required for the shell, especially for the small stones. The density of the material required was calculated and is presented in Table 3. A ratio of 1:2 parts resin to coarse Al_2O_3 (Sample Number 11) was selected for the small and medium tracers to maximize density. To save costs, a ratio of 1:1:2 parts gravel to resin to coarse Al_2O_3 was selected for the large stones (Sample Number 13).

Table 3 - Fabricated density required

Stone Size	Total Volume (mL)	Stone Density (g/ cm^3)	Fabricated Material Density Needed (g/ cm^3)	Fabricated Material Sample Number
Small	48	2.65	2.83	11
Medium	99	2.66	2.74	11
Large	563	2.54	2.55	13

In addition to measuring the densities of the various ratios of materials, the durability of the different compositions was assessed. A cement mixer was used to simulate bedload transport; the fabricated samples were loaded into the cement mixer with water and other natural stones. The cement mixer was run on at 20 rpm for 1 hour, which is comparable to a travel distance of roughly 1.8 km. The stones were visually inspected for cracks or fractures and the weight of each sample was recorded before and after testing. The visual inspection did not identify any cracks or fractures on any of the tested samples and none of the samples significantly varied in mass (Table 2).

3.3 Quality Control Tests on Tracer Deployment in the Field

Three sizes of synthetic traces were seeded; small, medium and large, a summary of each size group's characteristics is presented in Table 4. A total of 304 tracers were seeded across three riffles (168 small, 85 medium and 52 large).

Table 4 – Real Stone Characteristics

Type	Average a-axis (mm)	Average b-axis (mm)	Average c-axis (mm)
Small	58.45	39.40	38.00
Medium	86.00	61.00	35.30
Large	134.0	112.0	64.60

The average dimensions and shape of the tracers were compared to the size and shape of the real stones (Table 5). The tracers are on average larger than the real stones. Since the mold is made from a flexible silicone, the increased size is likely a result of overfilling the molds and/or the pressure applied to the

molds during the drying time. Depending on the side that the additional pressure was placed, the expansion or reduction could occur on a different axis.

Table 5 – Tracer Characteristics Compare to Real Stones

Length (mm)	Small			Medium			Large		
	Real	Fabricated	Δ*	Real	Fabricated	Δ*	Real	Fabricated	Δ*
a-Axis	58.45	58.08	-1%	86.00	85.26	-1%	134.0	140.69	5%
b-Axis	39.40	50.74	29%	61.00	63.78	5%	112.0	118.24	6%
c-Axis	38.00	41.58	9%	35.30	42.06	19%	64.60	63.84	-1%

*Negative numbers indicate a decrease in size from real stone to fabricated stone

The densities of the tracers were compared to the density of the real stones from the field. The small and medium tracers are on average less dense than the real stones, while the larger tracers have similar densities when compared to the real stone (Figure 24). Additionally, the variability of densities decreases with size of the stone.

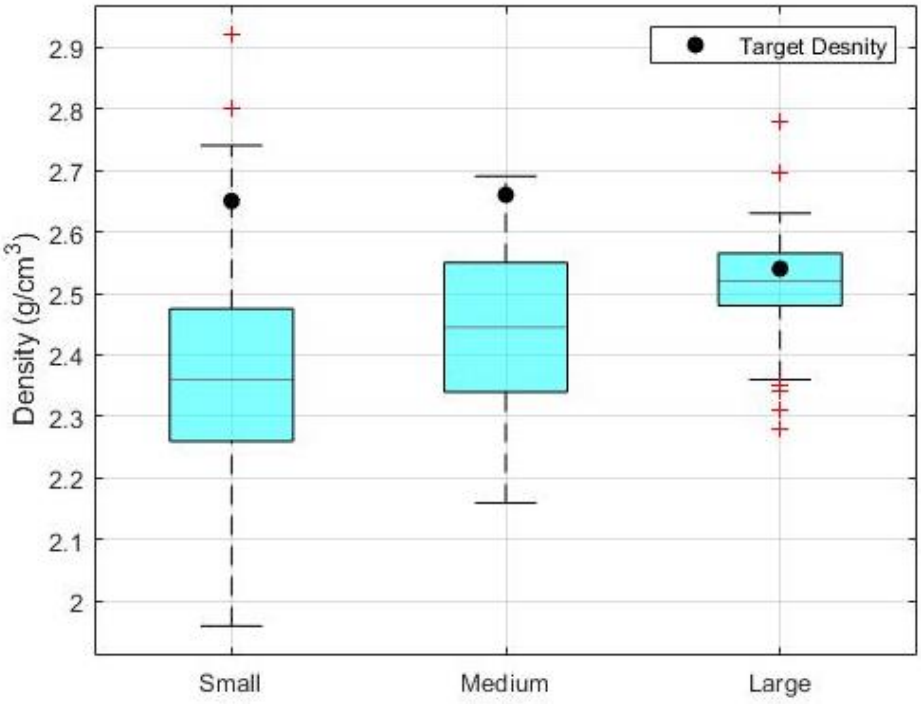

Figure 24 - Comparison between the tracer densities and the target density for each size of stone

The densities of the tracers are similar to those reported by Cassel et al. (2016), who reported an increase in travel velocities of synthetic versus natural stones as a result of stone shape and density. They also concluded that there were no systematic differences in the travel behavior between fabricated and real stones (Cassel et al. 2016). As a recommendation, flume investigations should be conducted to determine whether the mobility of wobble and non-wobblestones is significantly different.

3.4 Burial Depth Measuring Apparatus

To measure the burial depth of the wobblestone tracers, the RFID stick antenna was modified to determine the burial depth of a tracer in the field. A sliding mechanism was created to smoothly move the antenna vertically up and down above the buried stone. A ruler and needle were attached to the sliding mechanism to indicate the burial depth. Two different prototypes were created: one with a bent AEA580 stick antenna with GES3S Data Tracer Reader, Oregon RFID Inc. (non-modified) and one with a modified straightened antenna (same make and model).

3.4.1 Prototype 1 – Bent Antenna

To test the accuracy of the measuring device, a series of blind tests were conducted. The initial testing location was located outside in fully saturated sand. The trials consisted of one person (the hider) burying either a wobblestone or a synthetic stone containing a fixed RFID tag. The second person (the finder) would then locate the stone in the horizontal plane with the antenna, indicate its position with a flag and estimate the burial depth using the measuring device. The hider would then locate the stone and record the actual depth and the positioning error in the horizontal plane. The hider would then hide a new stone; the type of stone, rotation, burial depth and location was randomly varied and unknown to the finder. The actual burial depth versus the measured burial depth was compared to determine the accuracy of the measuring device (Figure 25).

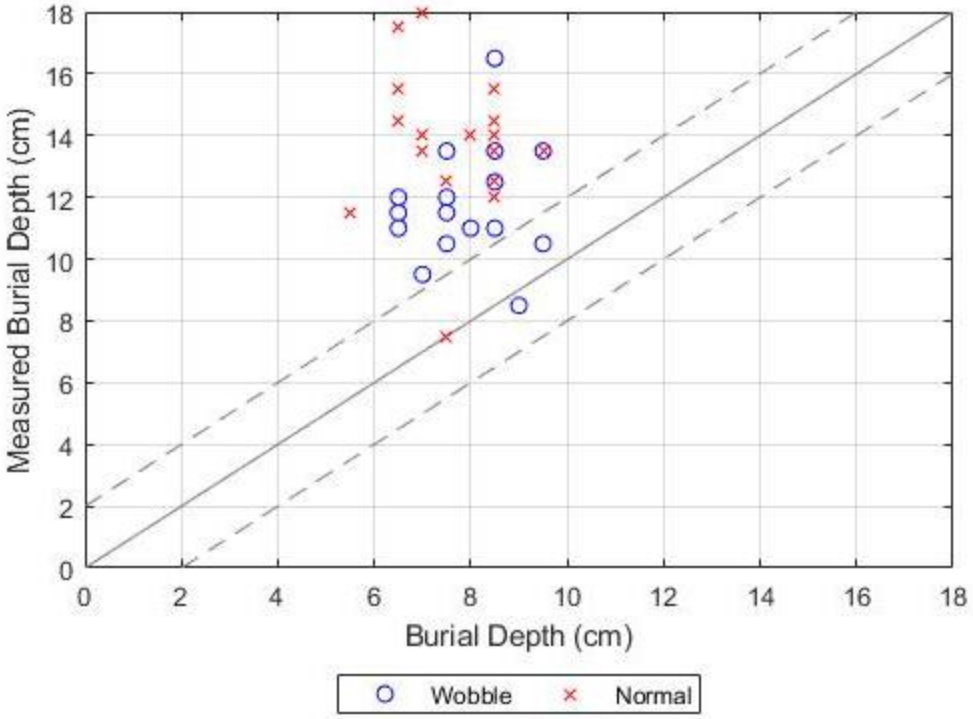

Figure 25 - Depth measurement comparison for prototype 1

For this antenna prototype the wobblestone did not perform any better than the normally tagged fabricated stone. This result indicated that either the wobblestone offered no improvement over a fixed RFID tracer or that the measuring device was not accurately recording the burial depth. Figure 26 shows a conceptual diagram of how a slight horizontal positioning error with a bent antenna could result in inconsistent burial depth measurements. To assess whether an error was introduced due to the bend of the antenna, the antenna was straightened, and the test was repeated.

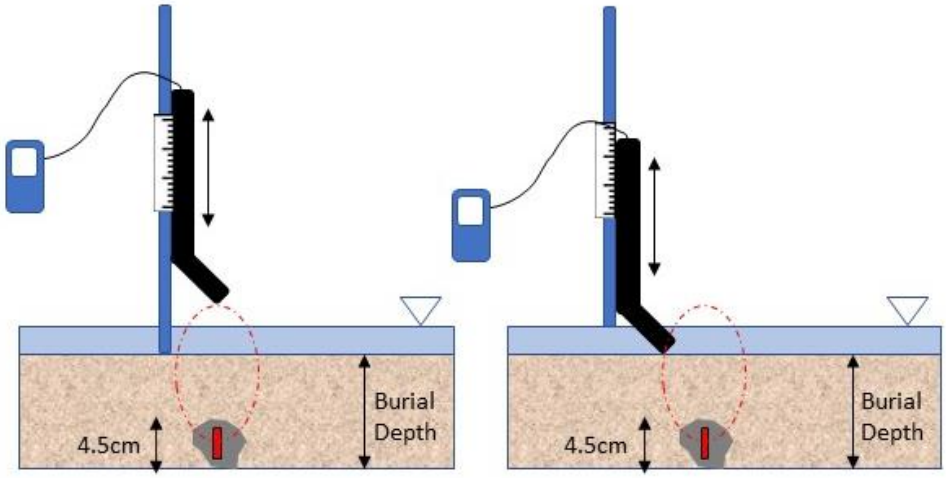

Figure 26 - Example of how the bend in the antenna can impact burial depth measurement

3.4.2 Prototype 2 – Straight Antenna

To remove the bend in the antenna, the PVC tubing that holds the RFID antenna was cut and then fixed in a straightened position. Conceptually it was reasoned that this change would reduce the sensitivity of the design to horizontal positioning errors (Figure 27). Blind tests, largely following the procedure described above, were then conducted to determine the accuracy of the measuring device. Unlike the previous tests, both saturated and unsaturated conditions were tested in a lab setting.

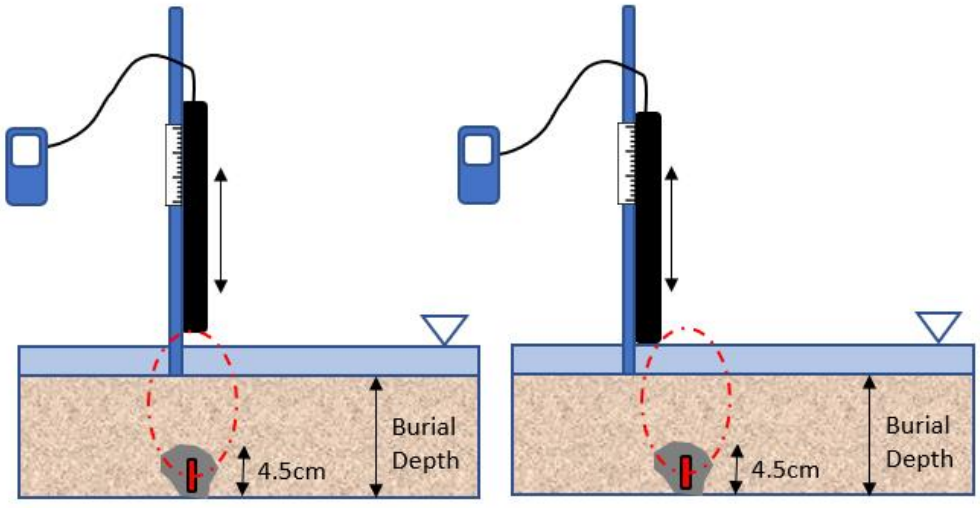

Figure 27 - Sample of how the straightened antenna improves burial depth measurements

In contrast to the results from the bent antenna, the measuring device was able to determine the burial depth of the wobblestones in both saturated and unsaturated conditions within 2 cm (Figure 28 and Figure 29). This result differs from the 1 cm accuracy reported in Papangelakis et al. (2019). There was no significant improvement in the horizontal accuracy between the wobblestone and the normal stone (Figure 30). However, the normal stone was not able to be located when buried six times as opposed to the wobblestone that was only unable to be located two times. This suggests the potential for increased recovery rate of buried tracers.

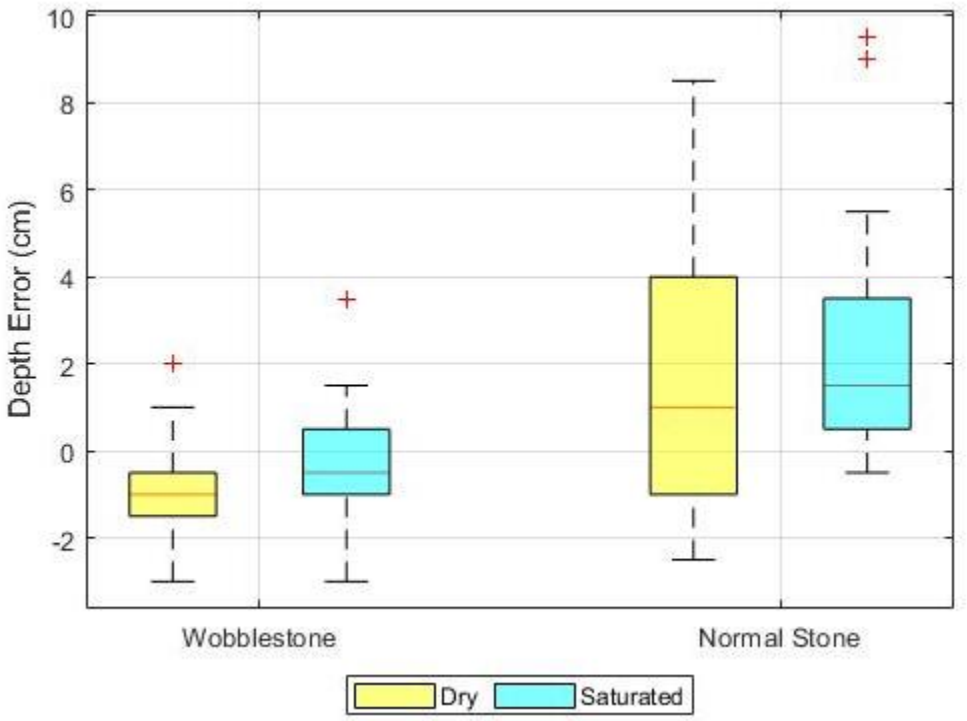

Figure 28 - Depth error comparison

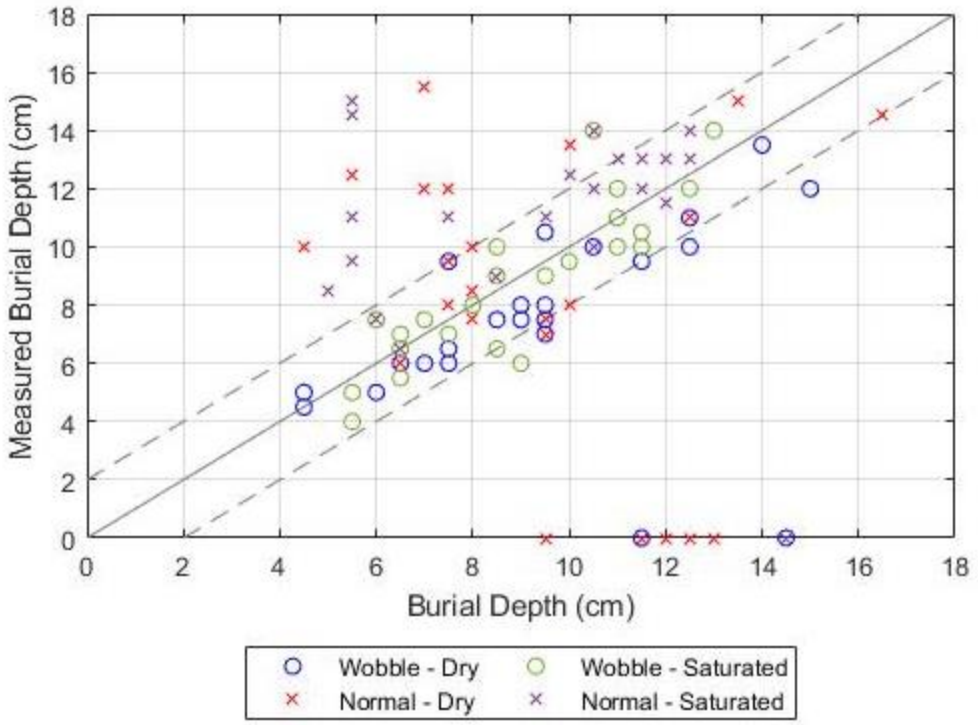

Figure 29 - Accuracy of prototype 2

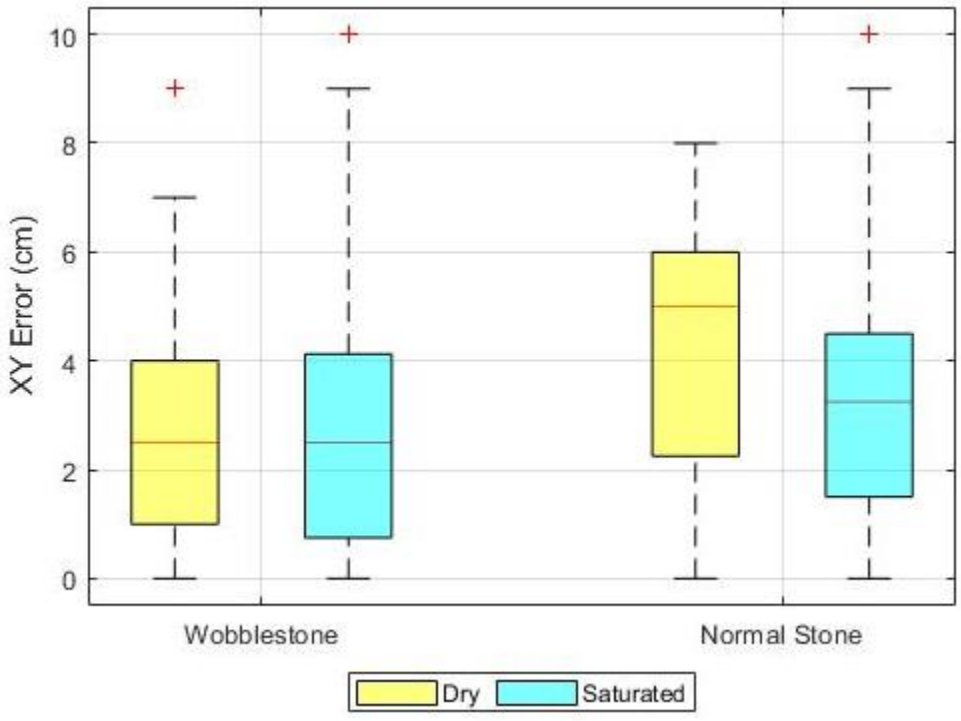

Figure 30 – Horizontal error comparison

3.5 Field Testing

A field test was conducted to determine the accuracy of buried stone location estimates in a field setting. The stones were seeded in June 2018 and tracked in May 2019. Of the 152 tracers seeded, 134 were found in May 2019 and of those 43 were determined to be buried. The buried depth of the tracers was assessed using the measurement device described in Section 3.4.2. The tracers were then dug up and the actual burial depth was recorded. It was noted that the actual burial depth measurement was difficult to determine because of the saturated conditions and uneven ground. The measured vs actual burial depth is presented in Figure 31.

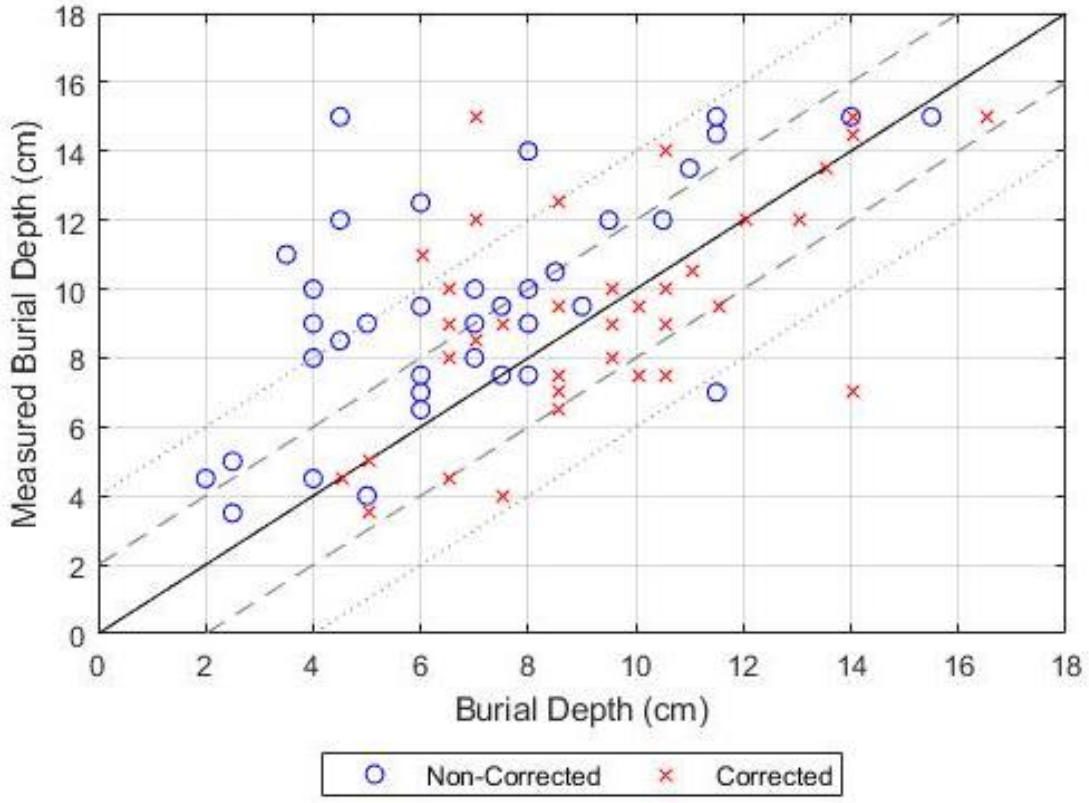

Figure 31 - Comparison of measures and actual burial depth

On average the measured burial depth overestimated the actual burial depth by approximately 2.5 cm. This offset error could be a result of the inaccurate measurement of the actual burial depth. It was difficult to uncover the tracers in the field and measure the actual burial depth. To correct for this offset, the actual

burial depth of the tracers was increased by 2.5 cm (red x's on Figure 31). With this modified actual burial depth, the majority of the measurements fall within the 4 cm error lines. Since the smallest tracers are on average 4.5 cm wide (b-axis) this was deemed an acceptable error for the depth measurement of tracers. Additional field experiments should be completed to improve the actual burial depth measurement process and to confirm the relationship between the offset and the particle size.

In addition, it is important to note that tracers were located at depths of up to 14 cm below the surface. This is likely only possible because the RFID tag was in the upright position, maximizing the detection zone. The detection of buried particles likely contributed to the high recovery rate (88%), which is higher than other studies that used 12 mm RFID tags, approximately 52% (Muirhead 2018).

3.6 Conclusions

Wobblestones show potential as a new sediment tracking technology that can determine the burial depth of stones and increase the recovery rates of tracers. Lab results indicated that burial depth could be determined with a +/-2 cm error. However, field tests indicated that the burial depth is only accurate to +/- 4 cm. Part of the difference between the field and lab measurements was because of the difficulty associated with identifying the true position of the tracers, therefore the true error is likely closer to the lab results. Both tests indicated an increase recovery rate compared to normally tagged tracer stones. More fieldwork should be conducted in order to improve the accuracy of the depth measurements.

Chapter 4 – Characterization of a Rural Semi-Alluvial River

4.1 Site Description

The study area is located on the western branch of Ganatsekiagon Creek, a tributary of Duffins Creek, in Pickering, Ontario (Figure 32). The total watershed area of Ganatsekiagon Creek is 13.1 km^2 and the primary land-use is agriculture, with less than 2% residential. However, within the next 5-years, new developments (Seaton Lands) are being constructed that will change the watershed's land-use to approximately 43.2% residential (The Sernas Group 2013). This change in land-use is likely to result in increased stream power that could impact the habitat of Redside Dace; an endangered species native to the study area (The Sernas Group 2013).

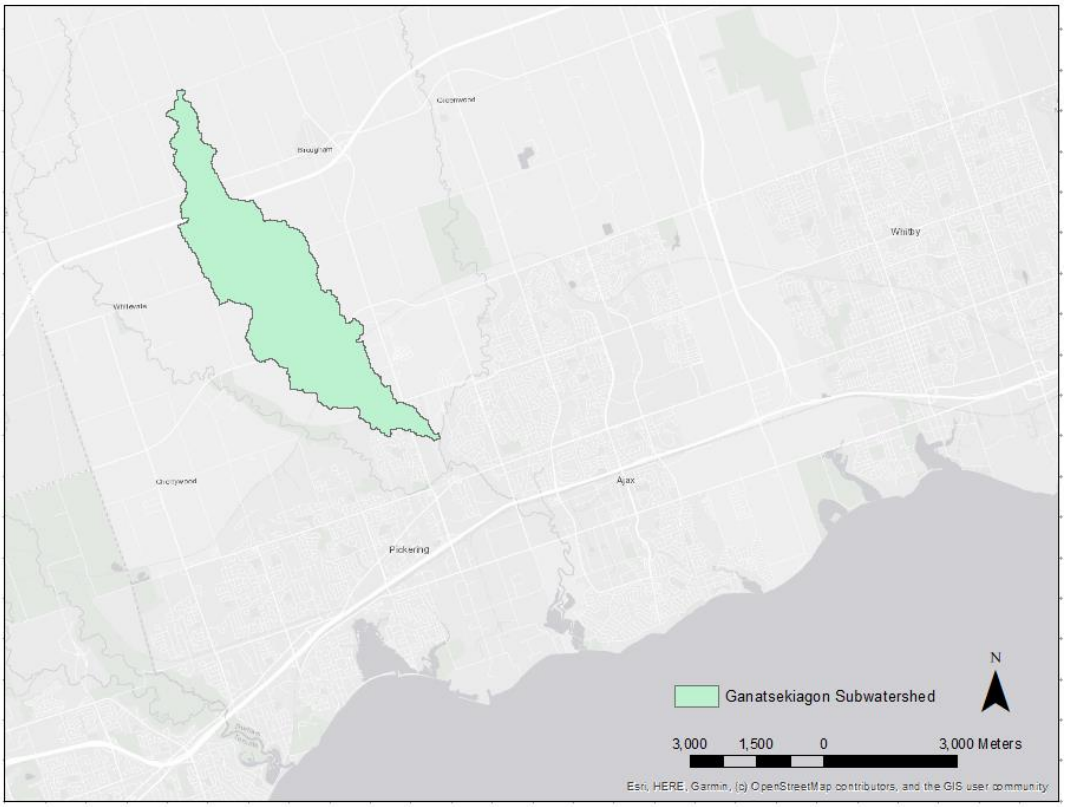

Figure 32 - Ganatsekiagon Creek subwatershed

The study site was selected based on its sensitivity to increased imperviousness, site reconnaissance and ease of access. An ArcGIS tool that was developed by the research group was used to help identify areas that will be sensitive to changes in land cover (Ghunowa 2017). This was done by comparing the stream power under the current land-use conditions to the proposed future development. Figure 33 shows how the existing development scenario could lead to large increases in stream power as a result of increased imperviousness. In addition, Seaton Lands will include five new stormwater management facilities that will outlet into the west branch of Ganatsekiagon Creek (The Sernas Group 2013). The new outlets could further impact the future hydrology and hydraulics in the study area and monitoring their impact is of interest to the research group and the Toronto Region Conservation Authority.

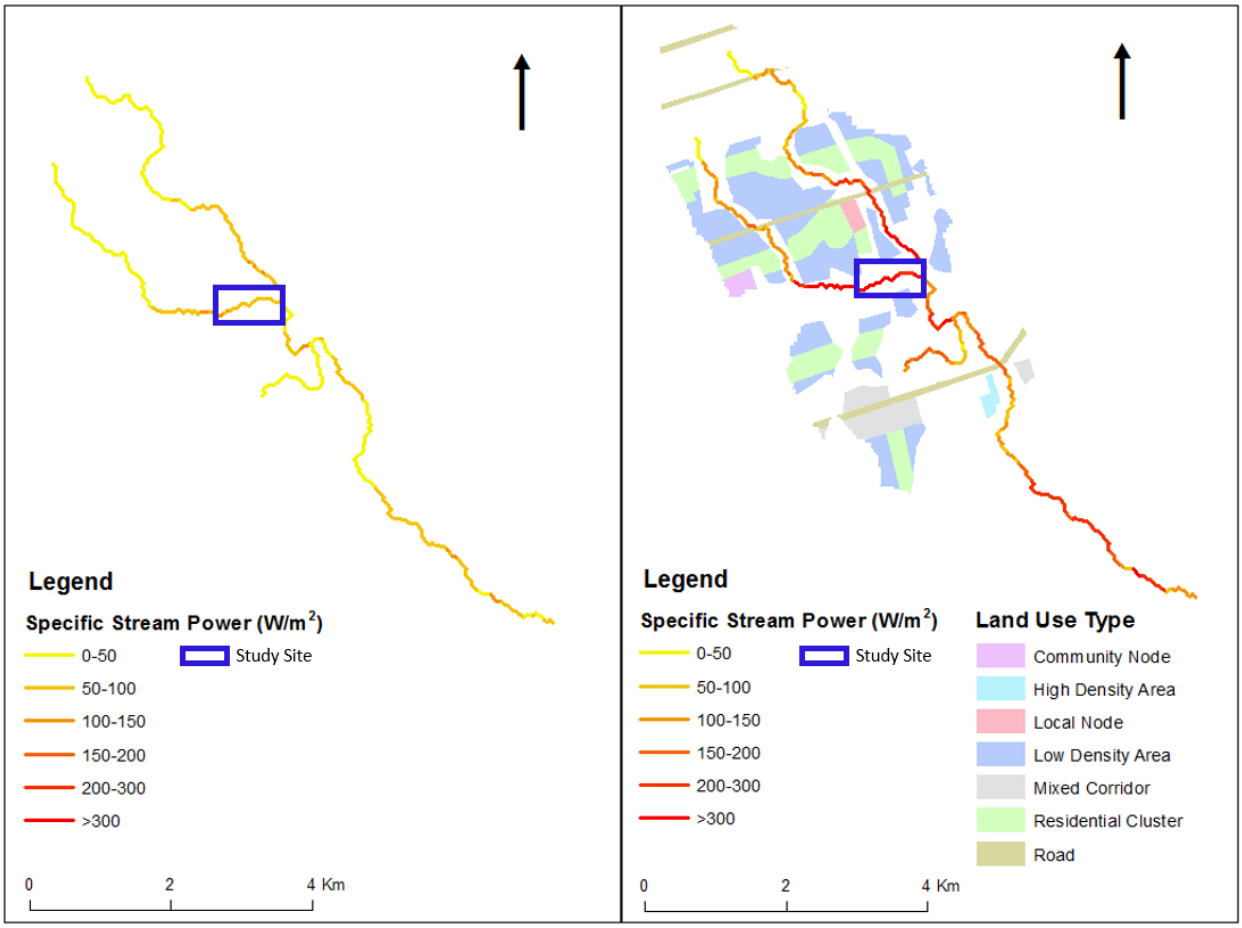

Figure 33 - Specific stream power before and after urbanization

The chosen site has an underlying geology of Halton Till and Newmarket Till, which causes the system to be semi-alluvial in nature. The upstream site is located on a reach with an exposed till bank that is introducing coarse gravel and cobble sized particles into the system as the wall actively erodes (Figure 34).

Figure 34 - Exposed Till Wall at the Upstream Seeding Site

4.2 Sediment Link Identification

To identify the location of sediment links across the study area, a detailed longitudinal profile and spatially distributed sediment distributions were required. A Sokkia total station was used to survey the top of bank, bottom of bank, thalweg, bar outlines and bar high points in a local coordinate system. A series of benchmarks were installed across the study area and were re-surveyed in global coordinates with an RTK GPS. The benchmarks were used to transform the remainder of the surveyed data into a global coordinate system.

A series of pebble counts were completed on riffles in the reach to characterize the longitudinal distribution of sediment sizes. The “modified” Wolman method was used to ensure sediment was selected and measured in an unbiased manner (Leopold 1970; Wolman 1954). The b-axis of at least 100 stones was measure across each riffle; a ‘zig-zag’ sample pattern was used to ensure all locations across the riffle were sampled. The stones were selected by taking a step and blindly touching a stone next to the left toe of the individual performing the pebble count. If material was touched that was less than 2 mm in size, it was identified as either fine gravel, sand or fines and recorded in a separate column (not included in the minimum 100 stones).

Two sediment links were identified in the study area; the sediment links are visible when the spatial variability in grainsize is plotted against the longitudinal profile of the study area. The hollow circles indicate the five largest stones recorded in each pebble count while the dashed and solid lines show the D_{75}, D_{25}, and D_{50}, respectively. The trend of the five largest stones indicate two downstream fining patterns (red arrows). However, this trend is not nearly as apparent when comparing the D_{50} values across the study area. The two sediment links are also identifiable by the scalloping longitudinal profile; Figure 35 shows how the profile is concave as the particle size decreases (green lines).

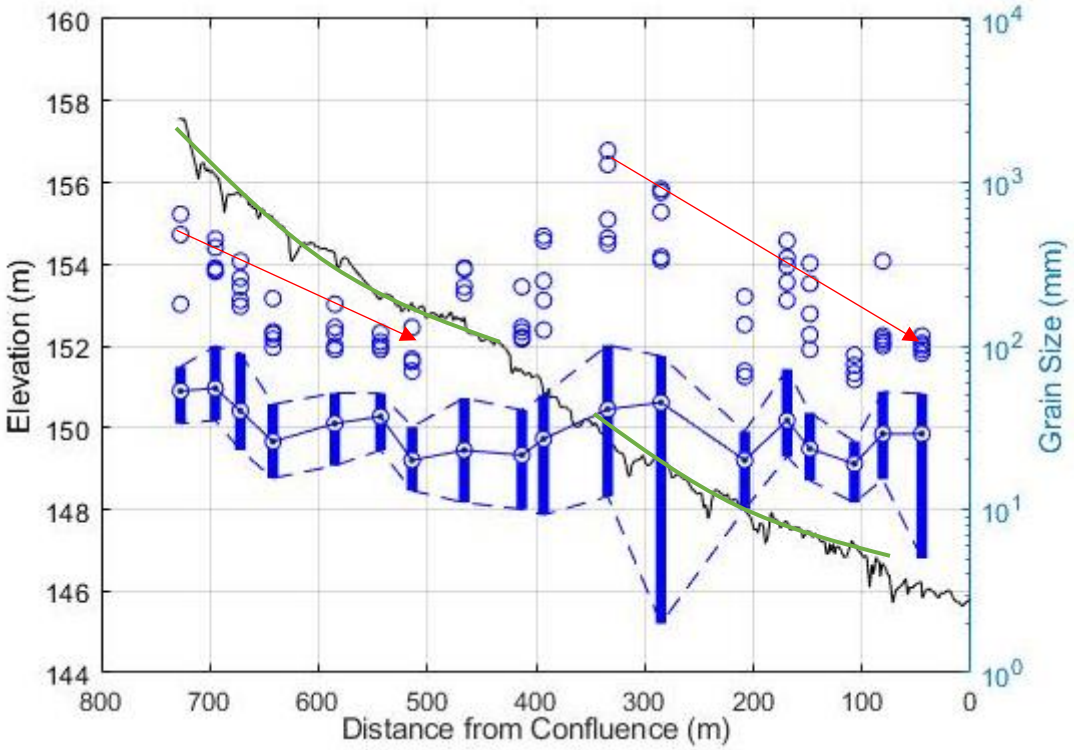

Figure 35- Longitudinal profile of the thalweg elevation and grainsize distribution in the west branch of Ganatsekiagon Creek

Ongoing development in the watershed could cause a shift towards a higher stream power environment. It is hypothesized that the coarser material in the upper portion of the sediment links could act as a protective barrier against bed erosion but could cause significant bank erosion and widening of the channel. This agrees with the first stage of the proposed evolution model for SAGT rivers presented by Bevan et al. (2018). As the active channel widens, the specific stream power should decrease until bank erosion is no longer possible. However, the reaches with finer bed material won't be protected against bed erosion and could experience an overall increase in channel slope and a further increase in stream power. This would theoretically continue until the knick point migrates up or down stream or coarser sediment is introduced into the system that protects the bed from further erosion. Continual monitoring of the identified sediment links should continue to confirm this hypothesis.

4.3 Hydraulics

To monitor the hydraulics of the study area, two water monitoring stations were installed. For each station a Hobo U20 Water Level Logger (model number U20-001-0X) was placed inside of a metal housing that was secured in the bed of the river. Water pressure and temperature readings were recorded at time intervals ranging from 2 minutes to 10 minutes, Table 6 summarises the recording time periods for each monitoring location. The gauge pressure was calculated by subtracting the barometric pressure measured using a gauge that was installed in a tree near the site and converted into an equivalent depth of water. The elevation of each pressure transducer was surveyed with a Sokkia total station and was used to determine the surface water elevation.

Table 6 - Summary of hydraulic data collected during the 1 year study period

GCrk50 (Downstream)			
Start Time	**End Time**	**Interval**	**Comment**
2018-04-14	2018-08-15	2 minutes	Installed on April 14, 2018
2018-08-15	2018-12-01	5 minutes	Changed to decrease field visits
2018-12-01	2019-03-15	10 minutes	Changed to decrease field visits over winter
2019-03-15	2019-04-10	5 minutes	Changed to increase data quality over spring freshet
GCrk60 (Upstream)			
2018-06-07	2018-08-15	2 minutes	Installed on June 6, 2018
2018-08-15	2018-12-01	5 minutes	Changed to decrease field visits
2018-12-01	2019-04-19	10 minutes	Changed to decrease field visits over winter
2019-04-19	2019-05-24	5 minutes	Changed to increase data quality over spring freshet

The velocity for each time step was determined using the Keulegan equation:

$$V = 5.75 \log_{10}\left[\frac{12.2R_H}{k_s'}\right] \times \sqrt{g \times S_o \times R_H} \quad (8)$$

where V is the velocity, R_H is the hydraulic radius of the flow area based on the cross section of each gauge location (Figure 36), g is gravitational acceleration (9.81 m/s^2), S_o is the bed slope, and k_s' is a roughness coefficient equal to $2.8 \times D_{84}$ (López and Barragán 2008).

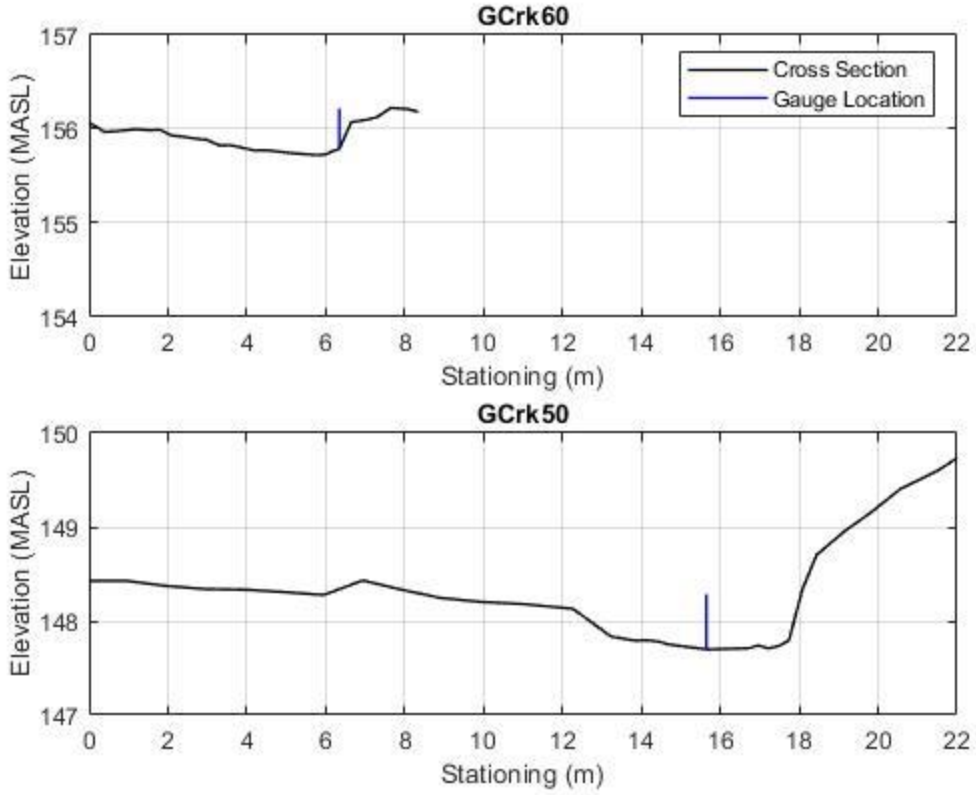

Figure 36 - Gauge cross sections and gauge location (looking downstream)

The number of high flow events within the study period that had the potential excess stream power to cause transport of the various tracer sizes was determined by calculating a critical water surface elevation. A dimensionless critical shear stress of the D_{50} (τ^*_{c50}) of each site was estimated as 0.047 (Buffington and Montgomery 1997). The dimensionless critical shear stress for each tracer size class (τ_{c_i}) was then estimated by applying a hiding function modifier (H_i). τ_{c_i} for each size class was calculated by rearranging the Shields equation:

$$\tau_{c_i} = (\tau^*_{c50} \times H_i) g(\rho_{sed} - \rho_{water}) D_i \quad (9)$$

where g, ρ_{sed}, and ρ_{water} are equal to the gravitation constant (9.81 m/s^2), the density of the tracers (2,600 kg/m^3), the density of water (1,000 kg/m^3), and H_i is a hiding function, developed by Egiazaroff (1965) as follows:

$$H_i = \frac{\log_{10}[19]}{\log_{10}\left[19\frac{D_i}{D_{50}}\right]} \quad (10)$$

A rating curve for each site was created to determine the corresponding water surface elevation to the critical shear stress for each tracer size class (Figure 37). An event is defined when the water level exceeds the critical water surface elevation and ends once it decreases to below the critical water surface.

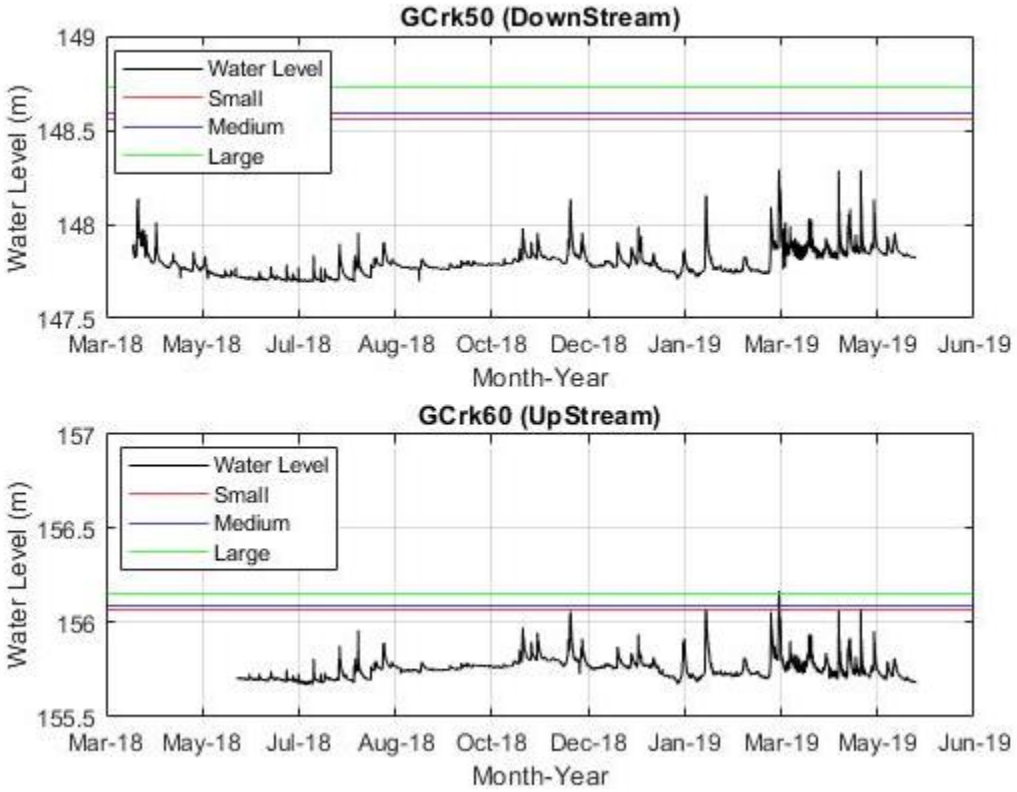

Figure 37 - Critical water surface elevation for each tracer compared to the hydrograph at each site

The difference between the baseflow and critical elevation between the two sites is largely a product of the bed slope, which is 0.019 in the upstream reach, and 0.010 the downstream slope. No events were detected at the downstream site that exceeded any of the tracer sizes water surface elevation thresholds. One event occurred at the upstream site that exceeded the water surface elevation for the small, medium, and large tracer size class. However, this event occurred over the winter (March 14th, 2019) when flow data is not reliable due to the presence of ice.

4.4 Sediment Tracking

4.4.1 Seeding Strategy

Tracers were seeded on upper portion of riffles using a pick and place method; a stone of similar size was removed from the bed and replaced with a tracer (Chapuis et al. 2015; Papangelakis, Macvicar, and Ashmore 2019). Tracers were placed at least 0.5 m apart to minimize the potential interference between neighboring RFID tags. The initial position of each tracer was surveyed with a Sokkia total station.

The tracers were monitored over a period of approximately one year (June 6th 2018 to May 24th 2019) using a similar methodology as that presented in Papangelakis, MacVicar, and Ashmore (2019). The new location of each tracer was determined using one of or a combination of two different types of RFID antenna readers: a stick antenna and a loop antenna. The stick antenna (AEA580 Antenna with a GES3S Data Tracer Reader, OregonRFID Inc.) has a detection radius of 0.2 m and was used to locate tracers in the majority of the study area where stones were deposited in close proximity to each other. The loop antenna (pole antenna and LF HDX Backpack Reader, OregonRFID) has a detection radius of 0.5 m and was primarily used to sweep the lower sections of the study reach where the tracers were more sparsely distributed. If a tracer was located with the loop antenna, the stick antenna was used to try to improve the precision of the estimated particle location. The location estimate of each tracer was recorded by surveying each tracers position with a Sokkia total station. If the stone was not visible on the bed surface of the river, a burial depth was recorded using the modified stick antenna as discussed in Section 3.4.2. The precision of each stone was recorded as either an X indicating the stone was visually on the surface, 20 cm if the stone was located with the stick antenna, or 1 m if the stone was located with the loop antenna. This information was used to determine the movement thresholds for each stone, see Section 4.4.2 for more details.

Three sizes of synthetic traces were seeded referred to herein as small, medium and large, as summarized in Table 7.

Table 7 - Tracer characteristics

Type	Average a-axis (mm)	Average b-axis (mm)	Average c-axis (mm)
Small	58	51	42
Medium	85	64	42
Large	141	118	64

A total of 304 tracers were seeded across three riffles (168 small, 85 medium and 52 large). Only 3 sizes of tracers were seeded to ensure a sufficient number of samples of each size class at each site. The number of tracers in each size class was based off reasoning presented in Papangelakis, MacVicar, and Ashmore (2019); that smaller size classes would have lower recovery rates and therefore needed higher seeded numbers to counteract the potential loss. The synthetic tracers were made following the procedure outlined in Chapter 3. The tracers used the 'wobblestone' RFID insert developed by Papangelakis et al. (2019) that enables the 12 mm PIT tag to remain in an upright position during transport. The main advantages to this type of tracer are increased recovery rates and the estimation of burial depth.

Tracers were seeded across two seeding sites referred to herein as the upstream and downstream sites (Figure 38). The upstream seeding site is half the width of the downstream site. To accommodate the difference in channel widths the stones were seeded across two riffles at the upstream site and one riffle at the downstream site. In addition, the upstream seeding sites have coarser material and are almost twice as steep as the downstream seeding site. A summary of the seeding riffle characteristics is presented in Table 8.

Table 8 - Seeding riffle characteristics

Site	Slope	Width (m)	D_{35} (mm)	D_{50} (mm)	D_{75} (mm)	D_{90} (mm)
Upstream-Upper	0.027	5	40	53	97	178
Upstream-Lower	0.019	5	27	40	91	133
Downstream	0.010	10	22	45	87	154

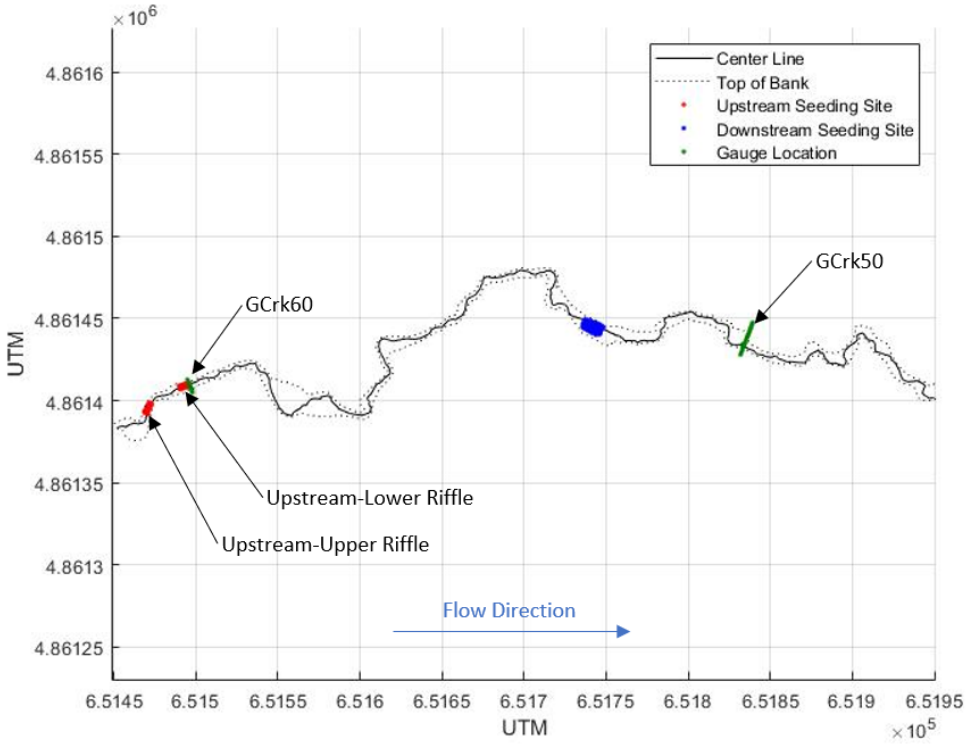

Figure 38 – Upstream and downstream seeding site and water level gauge location

Since the sediment size varies between the three seeding riffles, the three size classes of tracers represent different D_x at each site, where D_x is the diameter percentile of the size distribution. Table 9 summarizes the number of stones seeded on each riffle and the respective size class that the seeded material represents. Additionally, Figure 39 compares the grain size distributions of each seeding riffle to the tracer sizes.

Table 9 - Seeding Strategy

Size Group	Total Number	Upstream-Upper		Upstream-Lower		Downstream	
		Number	D_x	Number	D_x	Number	D_x
Small	168	42	D_{47}	42	D_{63}	84	D_{55}
Medium	85	21	D_{58}	21	D_{67}	43	D_{63}
Large	52	13	D_{82}	13	D_{88}	26	D_{85}

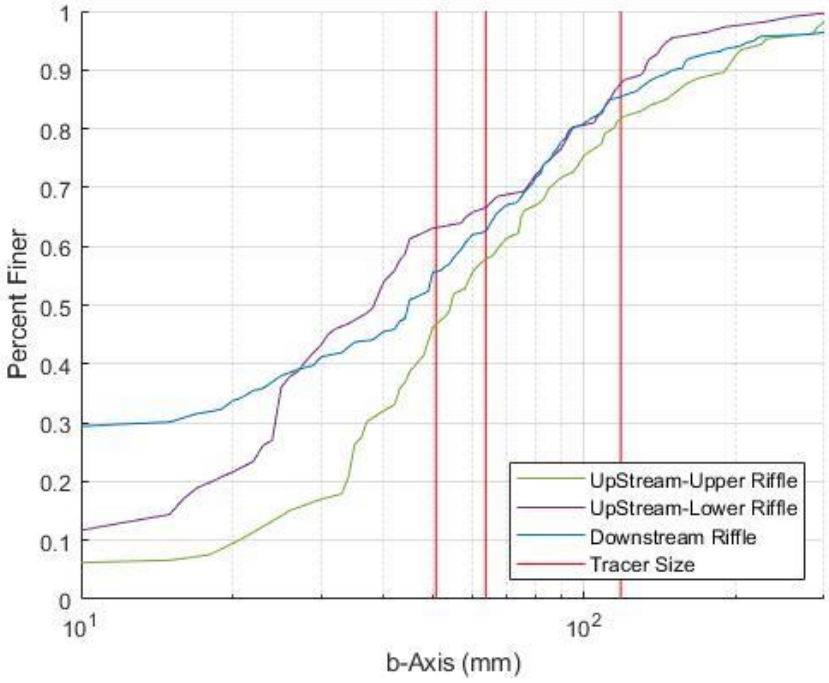

Figure 39 - Grain size distributions of the seeding riffles compared to the average tracer sizes

To ensure the tracers were a representative shape compared to the material at the study site, the shape of each tracer was compared to the size and shape of the bed material (Figure 40). Using the classification method presented by Zing (1935), the majority of the stones from the study area are classified as discs as are all three tracers.

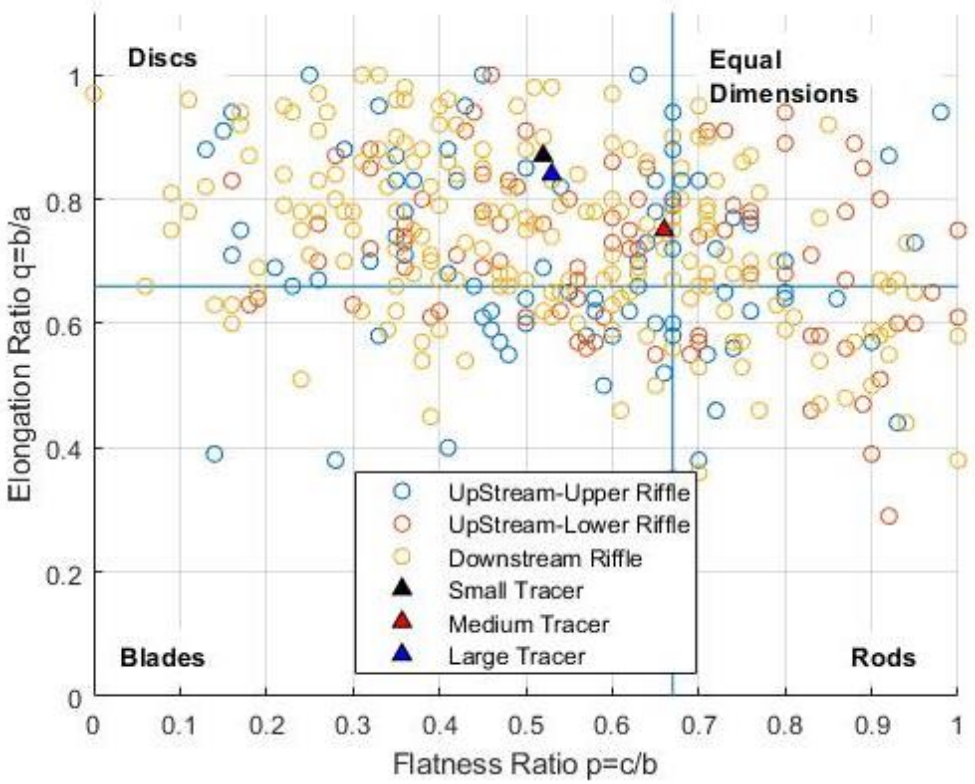

Figure 40 - Comparison of stone shape and tracer shape

4.4.2 Tracer Mobility and Travel Distance

The recovery rates for the two sites (upstream and downstream) were 88% and 75% respectively, which is higher than other studies that used 12mm RFID tags, approximately 52% (Muirhead 2018). Vázquez-Tarrío et al. (2018) reviewed several tracer studies and reported an average recovery rate of 81% for studies using PIT tags, which indicates that the recovery rates achieved in this study are comparable to this average. Additionally, all studies that were reviewed used 23mm PIT tags or larger except for MacVicar et al. (2015) who used 12mm tags for the smallest stones and reported lower recovery rates of this size class.

The travel distance of each stone was determined by projecting the initial and final locations of the tracer onto the centerline. The centerline distance between the projected points was assumed to be the travel distance of the stone and therefore assumes that the stones travel parallel to the centerline of the reach.

Stones are only considered to have moved if they move a larger distance than 0.5 m if they were found visually on the surface (marked with an X) or with the stick antenna, and 1 m if they were found with the loop antenna (Papangelakis, Macvicar, and Ashmore 2019).

The mobility fraction (p_m) was calculated based on the number of stones found at each site (n) and the number of stones that moved (m) as follows:

$$p_m = \frac{m}{n} \tag{11}$$

The 95% confidence interval of p_m was then calculated using the formula for a binomial confidence interval:

$$CI = z\sqrt{\frac{p_m(1-p_m)}{n}} \tag{12}$$

where z is equal to 0.975 for the 95% confidence interval (Macvicar et al. 2015; Papangelakis, Macvicar, and Ashmore 2019). The mobility fraction, p_m Equation (11) , for the upstream and downstream sites was 0.78 and 0.38, respectively, indicating that both sites experienced at least one above threshold event during the study period. All tracer size classes at both sites showed mobility during the study period (Figure 41).

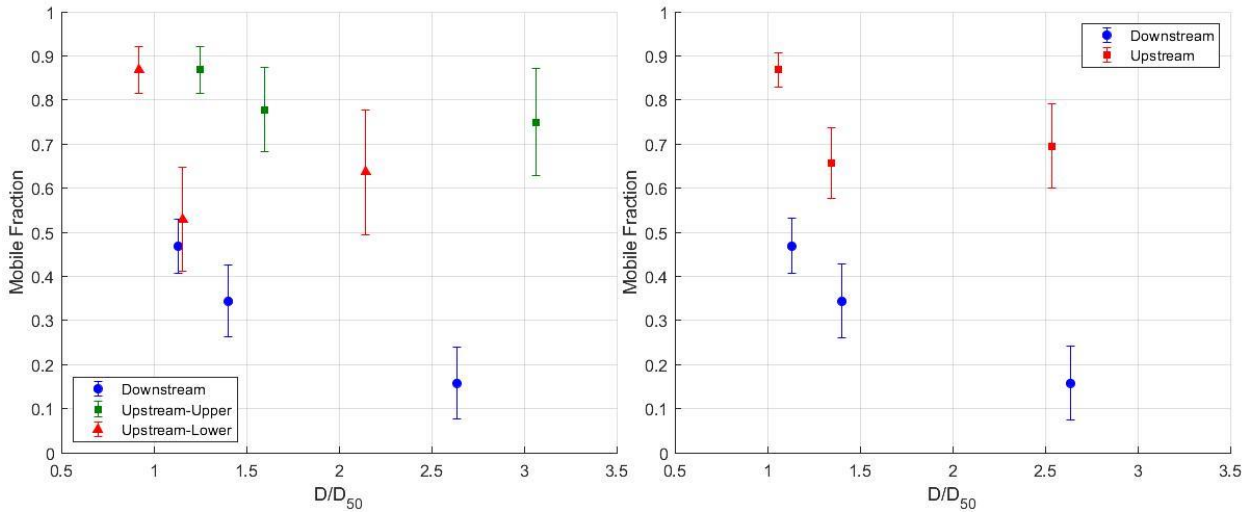

Figure 41 - Mobile fraction of tracers over the study period

Papangelakis, MacVicar, and Ashmore (2019) conducted a similar study on a lower portion of Ganatsekiagon Creek. They concluded that this system is subject to size-selective transport which is defined as larger grain sizes having lower mobility than small grain sizes (Ashworth and Ferguson 1989). The results presented in Figure 41 support conclusion for the downstream site but indicates equal mobility for all size classes for the upstream site. Equal mobility is typically characteristic of an urbanized watershed (Papangelakis, Macvicar, and Ashmore 2019). Further the upper riffle shows even stronger equal mobility tendencies with mobility fractions above 0.7 for all size classes. The lower riffle shows decreased mobility for the medium size class which could reflect impacts due to sediment hiding. Overall, this demonstrates that all sizes of tracers (that are similar sizes to the material that is introduced into the upstream sites from till erosion) are capable of being transported downstream.

It is generally accepted that the displacement of smaller tracers is larger than the displacement of larger tracers (Vázquez-Tarrío et al. 2018). However, several studies have reported that there is not apparent relationship between the size of a tracer and the travel distance (Milan 2013). The average travel distance ($\bar{L}$) was calculated as the geometric mean of the travel distances of each mobile tracer of the given size class (L). The geometric mean is used as opposed to the arithmetic mean because of the high degree

skewness in the travel length distribution (Macvicar et al. 2015; Papangelakis, Macvicar, and Ashmore 2019).

$$\bar{L} = 10^{\wedge}\left[\frac{\sum \log_{10}(L)}{\sqrt{n}}\right] \tag{13}$$

The 95% confidence interval of the average travel distance can be calculated as:

$$CI = 10^{\wedge}\left[\frac{SD_L}{\sqrt{n}}\right] \tag{14}$$

where SD_L is the standard deviation of the $\log_{10}$ travel distances of the stones that moved in the given size class. $\bar{L}$ ranges from 3.89 m to 17.7 m for the upstream site and 0.95 m to 4.32 m for the downstream site. Both upstream and downstream sites exhibit exponential decay of travel distance with grainsize (Figure 42).

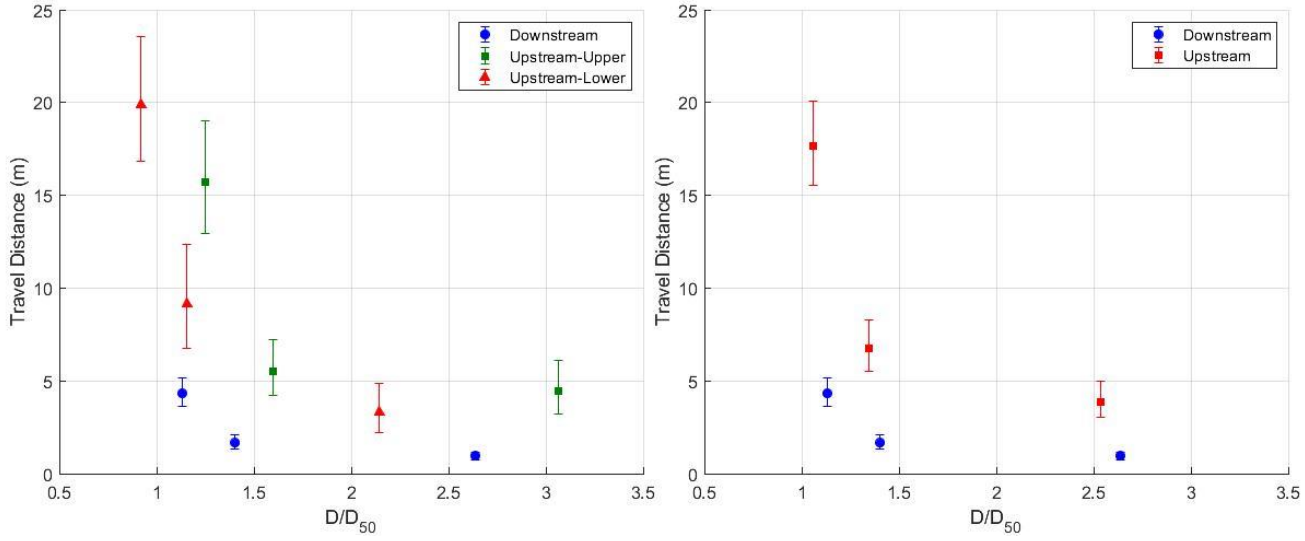

Figure 42 - Travel distance of tracers over the study period

Several relationships have been developed relating normalized travel distance $\left(\frac{\bar{L}}{\overline{L_{50}}}\right)$ to normalized grainsize distribution $\left(\frac{D}{D_{50}}\right)$. Church and Hassan (1992) proposed the following relationship for rivers that are constrained (finer material is fully mobile and the coarser fraction is partly mobile):

$$\frac{\bar{L}}{\overline{L_{50}}} = \left(1 - \log\frac{D}{D_{50}}\right)^{1.35} \tag{15}$$

where $\overline{L_{50}}$ and D_{50} are the geometric mean travel distance for the median grainsize and the median grainsize of the site (Church and Hassan 1992). Church and Hassan (1992) also proposed a power law relationship, Equation (16), to describe the relationship between grain size and path length in conditions where the coarser fraction is fully mobile, and all sizes are unconstrained (not influenced by other particles on the bed).

$$\frac{\bar{L}}{\overline{L_{50}}} = \left(\frac{D}{D_{50}}\right)^{-2.0} \tag{16}$$

Tracers that are loosely scattered on the surface of the bed should theoretically follow Equation (16). However if a pick and place method is used, the particles should be imbricated and Equation (15) should better describe their travel lengths. The last relationship used for comparison in this thesis was proposed by Vázquez-Tarrío et al. (2018) and is based off of data from 217 passive tracer experiments (from 33 scientific papers ranging in time from 1970 to 2016). This relationship plots similarly to Equation (16).

$$\log\frac{\bar{L}}{\overline{L_{50}}} = -0.26\frac{D}{D_{50}} + 0.26 \tag{17}$$

The data from this study has been plotted against the relationships identified above (Figure 43).

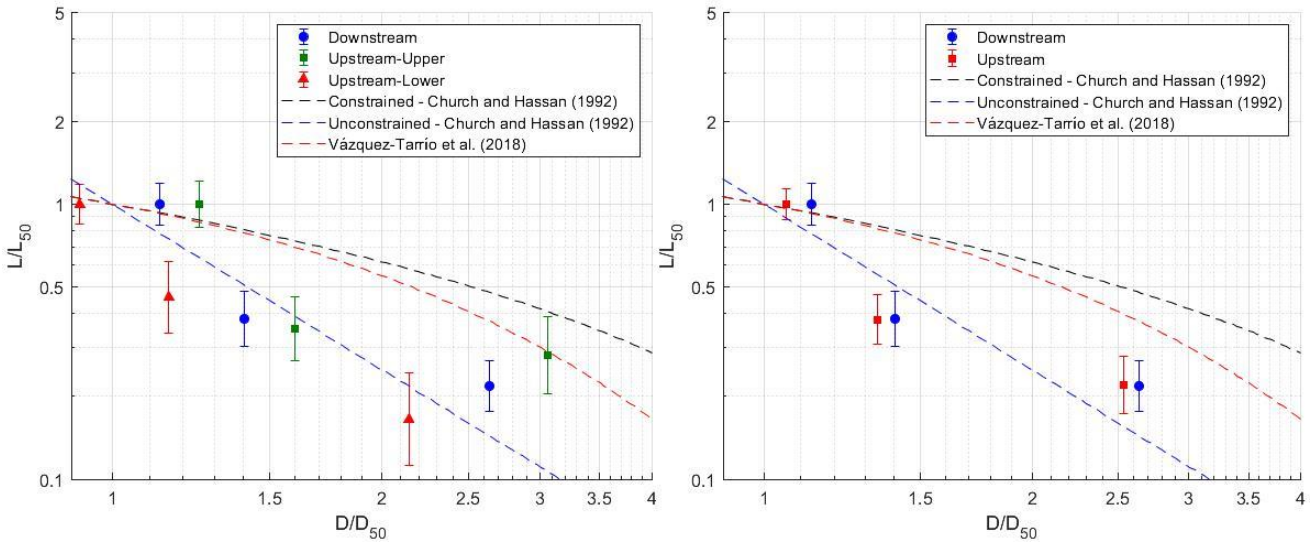

Figure 43 - Comparison of travel distances to relationships defined in other studies

The constrained relationship (Equation (15) proposed by Church and Hassan (1992) overestimates the travel distance of all tracers larger than the D_{50} in the study area. Similarly, the Vázquez-Tarrío et al. (2018) relationship overestimates the travel distances at all sites except for the upstream-upper riffle. It is therefore hypothesized that all sizes of tracers are unconstrained by the surrounding bed material. This hypothesis is confirmed because the normalized travel distances plot fairly closely to the Equations (16) and (17), which describe un-constrained conditions. This conclusion could be skewed because the particles were placed on the surface of the bed as opposed to being mixed into the active layer. Such a result would match with what has been found, for instance, for the first movement of sediment tracers in an event immediately after seeding (MacVicar and Roy 2011). Subsequent floods may reveal that the transport distances tend to converge on what has been found in other sites. However, it is hypothesized that the sites are experiencing unconstrained sediment transport in a manner similar to ephemeral streams where material is loosely deposited on the surface and remains stationary until times of high flow (Church and Hassan 1992).

Both sites were selected because they were close or at sediment sources where active bank erosion was contributing a wide range of particle sizes into the creek. The winter melts in this case were sufficient to

mobilize this material. Longer term studies are needed to monitor these types of systems, particularly during winter and spring freshets.

4.4.3 Tracer Burial Depths

At the end of the test period, particles of all three size classes were found to be buried. Overall 54 of 294 recovered tracers were buried, 11 from the downstream site and 43 from the upstream sites. Since higher mobility rates were observed in the upstream sites it was expected that more stones would be buried upstream as opposed to downstream. The likelihood of a stone being buried based on the size of the tracer tested using Equation 13 and 14 presented earlier in this thesis (Figure 44).

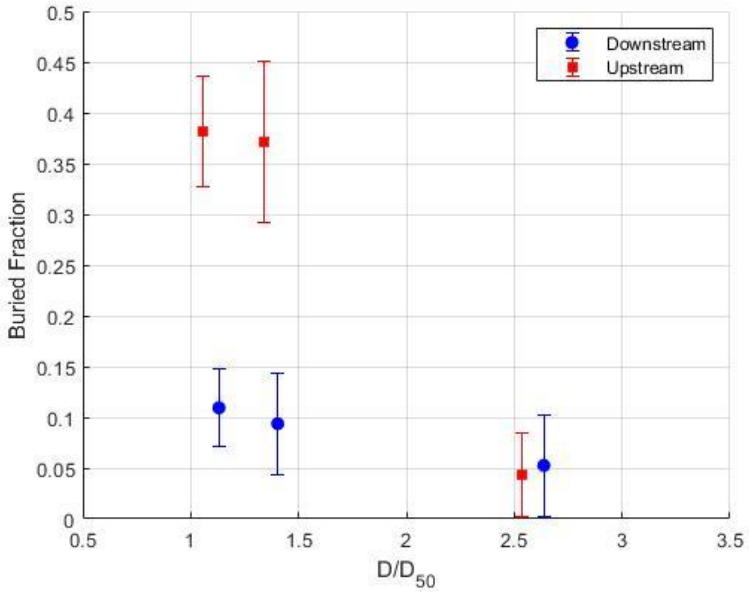

Figure 44 - Buried fraction based off of size

It appears that the small and medium tracers at the upstream site are more likely to be buried than the largest size tracer. However, at the downstream site there is no statistically significant impact on the likelihood of burial based on size of the tracer. Next, the possibility of a relationship between travel distance and burial depth was assessed (Figure 45). It was hypothesized that if a tracer was buried it would be less likely to become mobile.

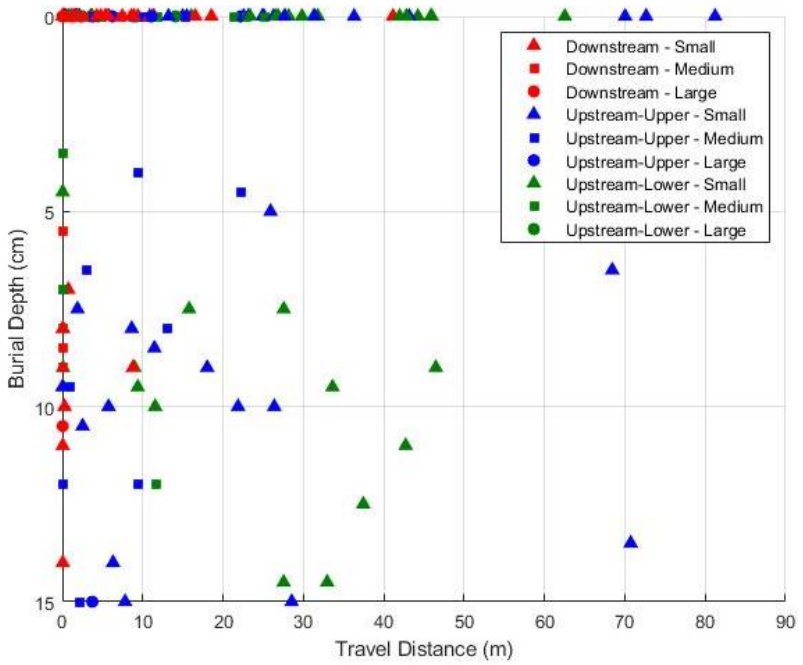

Figure 45 – Travel distance versus burial depth of tracers over the study period

However, there is no apparent relationship between burial depth and travel distance. These results indicate that the active layer at the upstream site was as deep as 15 cm in many locations, though not all given that many transported particles remained at the surface. Additionally, since the buried material at the downstream site does not appeared to be mobile, the downstream site could be a sediment deposition environment as opposed to a sediment production or transport environment.

Lastly, the relationship between the end location of the tracers and their burial depth was examined (Figure 46). It was hypothesized that if the tracer was deposited in a typical zone of deposition (bar or pool) that all tracers in that area would experience similar burial depths. However, there does not appear to be any relation between where the stones were deposited and how deeply they were buried.

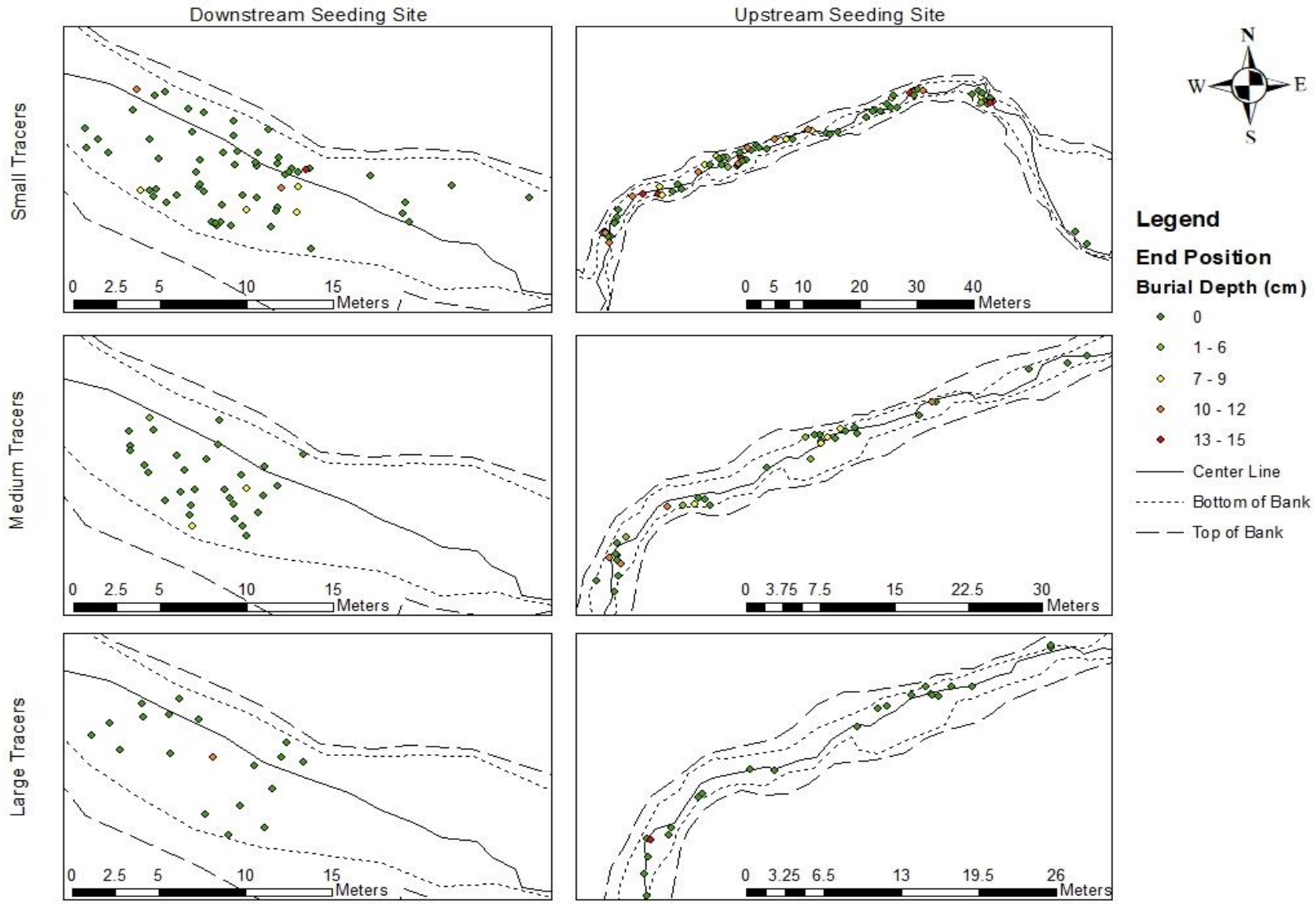

Figure 46 - Spatial distribution of buried tracer relative to their end position

4.4.4 Spatial Distribution of Tracers and Sediment Transport Rates

Figure 47 and Figure 48 show the spatial distribution of tracers across both seeding sites. Overall the upstream upper riffle shows bank to bank movement, while the upstream lower has movement on one side of the centerline and the downstream has moderate movement through the middle of the riffle. Tracers that were not found at the downstream site appear to be located in clusters. This suggests that either these tracers were moved downstream, which is unlikely because subsequent riffles were searched with the loop antenna and no tracers were found. Alternatively, the location of the tracers were masked due to signal collision, this could be avoided in future studies by placing the tracers further apart. Figure 48, indicated that at the downstream site the largest size of tracers barely moved and have simply shuffled their position within the seeded riffle, while in some cases the smaller particles have moved out of the seeded riffle.

At the upstream site, Figure 47 shows that the large tracers have not passed the subsequent riffle, while the smaller tracers have passed multiple riffles during the study period. Given that many particles on the upstream-lower riffle did not move, this suggests that that some tracers in motion were able to pass over or beside the stationary tracers and move far downstream. Additionally, the tracers appear to deposit in clusters on the riffles. An active width (w) of approximately 2.5 m was calculated based on Figure 47. This width can be used to estimate the sediment flux Q_s for the upstream site using equation:

$$Q_s = \frac{\overline{L_{50}}}{year} \times w \times d \times (1 - p) \tag{18}$$

where d is the average burial depth of 10 cm, $\overline{L_{50}}$ is equal to 29.16 m, and p is the porosity of the bed material was assumed to be equal to 0.27 (Frings, Schüttrumpf, and Vollmer 2011). This results in a Q_s for the upstream site of 5.30 m^3/year, this value is purely an estimate based on the field collected data and the described assumptions.

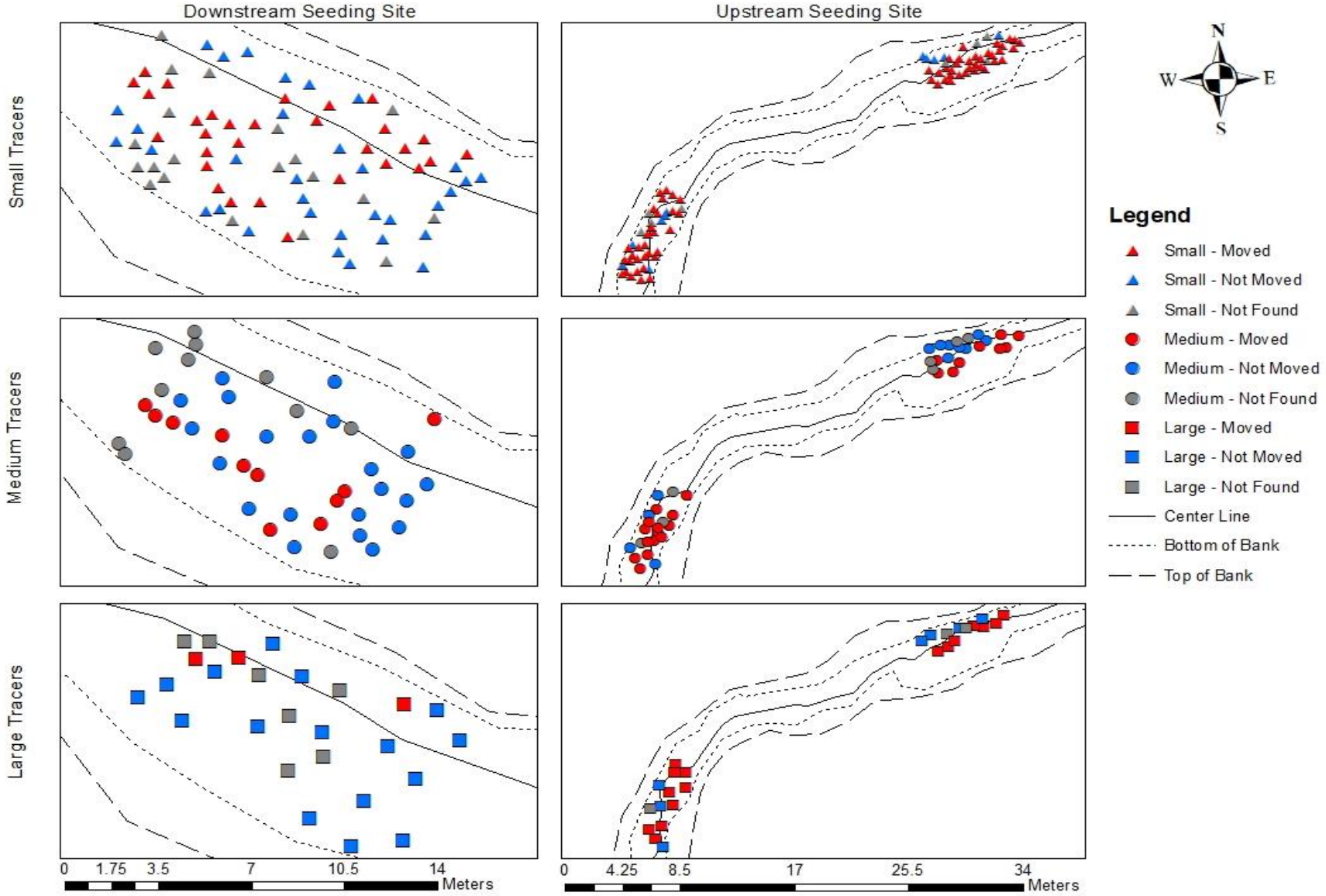

Figure 47 - Spatial view of tracers

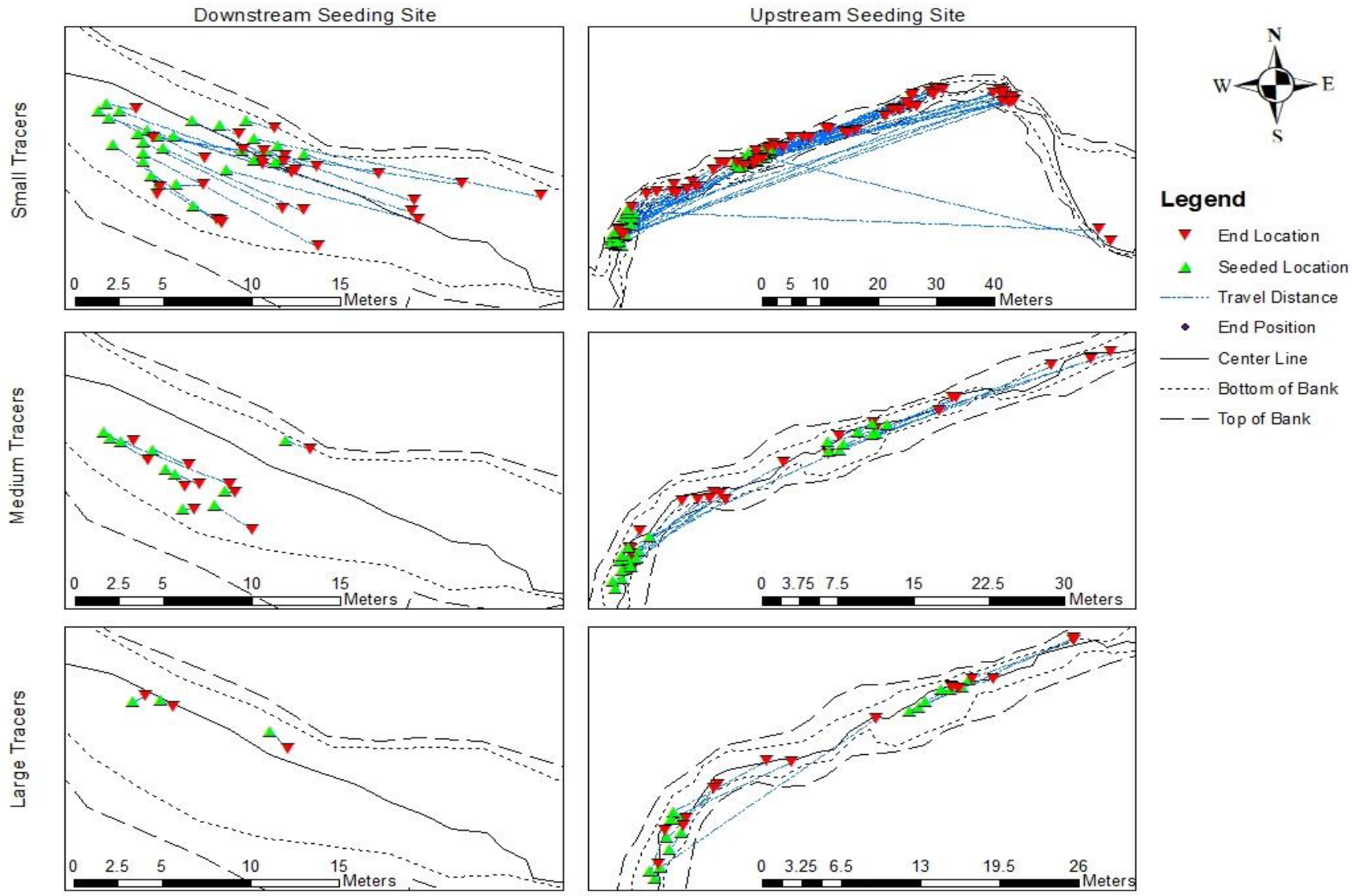

Figure 48 - Spatial view of moved stone

4.5 Conclusions

Two sediment links have been identified in the study area, these sites should be continually monitored through the current land development to verify the proposed hypothesis and the various evolution models proposed by others. Wobblestone tracers indicated that the upper site behaves as an unconstrained ephemeral system where the majority of the sediment transport occurs during winter snow melts and/or spring freshet. More research should be conducted to better understand the processes occurring in these systems during the winter period. Lastly, wobblestones have been proven to increase the recovery rates of smaller PIT tags and show promise in determining an estimated sediment flux.

Chapter 5 – Conclusions

Ganatsekiagon Creek is a semi-alluvial river located in Pickering Ontario that is of interest because the next 5 years it will see a rapid increase in urban-residential land-use (from 2% to 43%) which could impact the habitat of an endangered species. Since most of the current evolutionary models that describe the impact of urbanization on streams focus on the feedback between river morphology, hydraulics and sediment transport, it is important that these variables are quantifiable in real rivers (not just lab settings). Sediment transport can be characterized by measuring bedload transport which is typically quantified using one of the following methods: bulk sampling, indirect sampling or sediment tracking. However, none of these methods can fully quantify the rate of bedload transport as they are all missing different aspects of the process. This methodological deficiencies were used as motivation for the development of a new type of Radio Frequency Identification (RFID) tracer called a 'wobblestone' (Papangelakis et al. 2019).

Wobblestones show potential as a new sediment tracking technology that can determine the burial depth of stones and increase the recovery rates of tracers. Field tests indicated that the burial depth can be determined with an accuracy of +/- 4 cm, a change from the +/- 1cm accuracy presented in Papangelakis et al. (2019). Additionally, wobblestones have been proven to increase the recovery rates of smaller PIT tags and show promise in the estimation sediment flux. Additional fieldwork should be conducted in order to confirm the accuracy of the burial depth measurements. In addition, flume investigations should be conducted to determine the mobility difference between wobble and non-wobblestones.

Two sediment links have been identified on the western branch of Ganatsekiagon Creek. The field tracing results show that the gradients of bed slope and particle size lead to significant differences in sediment dynamics over short distances along the river. In the upper seeded site, the high mobility of coarse particle tracers and the strong negative relationship between particle size and transport distance is consistent with other unconstrained ephemeral systems. These patterns are consistent with the idea that this area is a source of bedload in the river and indicates that the steeper parts of the channel are in fact eroding

relatively rapidly and maybe sensitive to hydrologic changed in the watershed due to planned urbanization. The study area hydrology was difficult to assess because the transport appears to have occurred during winter snow melts and the spring freshet when the pressure gauges are not reliable due to ice buildup. It is recommended that more research is conducted to better understand the processes that occur during the winter period. The study site should remain the focus of future monitoring in order to verify the apparent differences in the mobility and transport through these semi-alluvial glacial till rivers and to assess their sensitivity and evolution as a result of urbanization.

Work Cited

Allan, Jonathan C., Roger Hart, and J. Vincent Tranquili. 2006. "The Use of Passive Integrated Transponder (PIT) Tags to Trace Cobble Transport in a Mixed Sand-and-Gravel Beach on the High-Energy Oregon Coast, USA." *Marine Geology* 232(1–2): 63–86.

Allmendinger, Nicholas E., James E. Pizzuto, Glenn E. Moglen, and Mikolaj Lewicki. 2007. "A Sediment Budget for an Urbanizing Watershed, 1951-1996, Montgomery County, Maryland, U.S.A." *Journal of the American Water Resources Association* 43(6): 1483–98.

Arnaud, F. et al. 2015. "Technical Specifications of Low-Frequency Radio Identification Bedload Tracking from Field Experiments: Differences in Antennas, Tags and Operators." *Geomorphology* 238: 37–46. http://dx.doi.org/10.1016/j.geomorph.2015.02.029.

Ashworth, Philip J., and Robert I. Ferguson. 1989. "Size-selective Entrainment of Bed Load in Gravel Bed Streams." *Water Resources Research* 25(4): 627–34.

Bagnold, R A. 1966. "An Approach to the Sediment Transport Problem From General Physics." *Geological Survey*. https://pubs.usgs.gov/pp/0422i/report.pdf.

Bevan, Vernon et al. 2018. "Enlargement and Evolution of a Semi-Alluvial Creek in Response to Urbanization." *Earth Surface Processes and Landforms* 11(43): 2295–2312.

Beylich, Achim A., and Katja Laute. 2014. "Combining Impact Sensor Field and Laboratory Flume Measurements with Other Techniques for Studying Fluvial Bedload Transport in Steep Mountain Streams." *Geomorphology* 218: 72–87. http://dx.doi.org/10.1016/j.geomorph.2013.09.004.

Bradley, D., and Gregory E. Tucker. 2012. "Measuring Gravel Transport and Dispersion in a Mountain River Using Passive Radio Tracers." *Earth Surface Processes and Landforms* 37(10): 1034–45.

Buffington, John M. 2000. "The Legend of A. F. Shields." *Journal of Hydraulic Engineering* 126(9): 718–23. http://ascelibrary.org/doi/10.1061/%28ASCE%290733-9429%282000%29126%3A9%28718%29.

Buffington, John M., and David R. Montgomery. 1997. "A Systematic Analysis of Eight Decades of Incipient Motion Studies, with Special Reference to Gravel-Bedded Rivers." *Water Resources Research* 33(8): 1993–2029.

Bunte, Kristin, Steven R. Abt, John P. Potyondy, and Kurt W. Swingle. 2008. "A Comparison of Coarse Bedload Transport Measured with Bedload Traps and Helley-Smith Samplers." *Geodinamica Acta* 21(1–2): 53–66. https://www.tandfonline.com/doi/full/10.3166/ga.21.53-66.

Camenen, B et al. 2010. "An Estimation of Gravel Mobility over an Alpine River Gravel Bar (Arc En Maurienne , France) Using PIT-Tag Tracers An Estimation of Gravel Mobility over an Alpine River Gravel Bar (Arc En Maurienne , France) Using PIT-Tag Tracers." *International Conference on Fluvial Hydraulics* (September): 953–60.

Cassel, Mathieu, Thomas Dépret, and Hervé Piégay. 2017. "Assessment of a New Solution for Tracking Pebbles in Rivers Based on Active RFID." *Earth Surface Processes and Landforms* 42(13): 1938–51.

Cassel, Mathieu, Hervé Piégay, and Jérôme Lavé. 2016. "Effects of Transport and Insertion of Radio Frequency Identification (RFID) Transponders on Resistance and Shape of Natural and Synthetic Pebbles: Applications for Riverine and Coastal Bedload Tracking." *Earth Surface Processes and Landforms* 42(3): 399–413.

Chapuis, Margot et al. 2015. “Coupling Channel Evolution Monitoring and RFID Tracking in a Large, Wandering, Gravel-Bed River: Insights into Sediment Routing on Geomorphic Continuity through a Riffle-Pool Sequence.” *Geomorphology* 231: 258–69. http://dx.doi.org/10.1016/j.geomorph.2014.12.013.

Chapuis, Margot, Christina J. Bright, John Hufnagel, and Bruce Macvicar. 2014. “Detection Ranges and Uncertainty of Passive Radio Frequency Identification (RFID) Transponders for Sediment Tracking in Gravel Rivers and Coastal Environments.” *Earth Surface Processes and Landforms* 39(15): 2109–20.

Charlton, Ro. 2008. *Fundamentals of Fluvial Geomorphology*. New York: Toutledge.

Chin, Anne. 2006. “Urban Transformation of River Landscapes in a Global Context.” *Geomorphology* 79: 460–87.

Church, Michael. 2002. “Geomorphic Thresholds in Riverine Landscapes.” *Freshwater Biology* 47: 541–57.

Church, Michael, and Marwan A. Hassan. 1992. “Size and Distrance of Travel Unsconstrained Clasts on a Streambed.” *Water Resources Research* 28(1): 299–303.

Dade, W Brian, and Peter F Friend. 1998. “Grain - Size , Sediment - Transport Regime , and Channel Slope in Alluvial Rivers.” *The Journal of Geology* 106(6): 661–76.

Dey, Subhasish. 2014. “Bed-Load Transport.” In , 261–326. http://link.springer.com/10.1007/978-3-642-19062-9_5.

Dingman, S. Lawrence. 2009. *Fluvial Hydraulics*. Oxford University Press.

Du Boys, P. 1879. “Let Rhone et Les Rivieres a Lit Affouillable.” *Annales des Ponts et Chaussees* 5(18): 141–95.

Dziadak, Krystyna, D Ph, Bimal Kumar, and James Sommerville. 2009. “Model for the 3D Location of Buried Assets Based on RFID Technology.” 23(June): 148–59.

Egiazaroff, L.V. 1965. “Calculation of Non-Uniform Sediment Concentration.” *Journal of Hydraulic Engineering* 92: 225–48.

Einstein, H.A. 1937. Eidgenoess. Tech. Hochsch, Zurich, Switzerland “Bedload Transport as a Probability Problem (in German).”

Ergenzinger, P., and J. Conrady. 1982. “A New Tracer Technique for Measuring Bedload in Natural Channels.” *Catena* 9(1–2): 77–80.

Ettema, Robert, and Cornelia F. Mutel. 2004. “Hans Albert Einstein: Innovation and Compromise in Formulating Sediment Transport by Rivers.” *Journal of Hydraulic Engineering* 130(6): 477–87. http://ascelibrary.org/doi/10.1061/%28ASCE%290733-9429%282004%29130%3A6%28477%29.

Ferguson, Robert I. 2003. “Emergence of Abrupt Gravel to Sand Transitions along Rivers through Sorting Processes.” (2): 159–62.

FISRWG. 1998. *Stream Corridor Restoration: Principles, Processes, and Practices*. papers2://publication/uuid/1CA00793-D230-43EE-8098-56B82A41B09D.

Ford, Murray R. 2014. “The Application of PIT Tags to Measure Transport of Detrital Coral Fragments on a Fringing Reef: Majuro Atoll, Marshall Islands.” *Coral Reefs* 33(2): 375–79.

Frings, Roy M., Holger Schüttrumpf, and Stefan Vollmer. 2011. “Verification of Porosity Predictors for Fluvial Sand-Gravel Deposits.” *Water Resources Research* 47(7): 1–15.

Frings, Roy M., and Stefan Vollmer. 2017. “Guidelines for Sampling Bedload Transport with Minimum Uncertainty.” *Sedimentology* 64(6): 1630–45.

Gallagher, Colman, Matthew Balme, and Nicholas Clifford. 2017. “Discriminating between the Roles of Late Pleistocene Palaeodischarge and Geological-Topographic Inheritance in Fluvial Longitudinal Profile and Channel Development.” *Earth Surface Processes and Landforms* 462(October 2017): 444–62. http://doi.wiley.com/10.1002/esp.4261.

Gasparini, Nicole M., Gregory E. Tucker, and Rafael L. Bras. 2004. “Network-Scale Dynamics of Grain-Size Sorting: Implications for Downstream Fining, Stream-Profile Concavity, and Drainage Basin Morphology.” *Earth Surface Processes and Landforms* 29(4): 401–21.

Ghunowa, Kimisha. 2017. “Spatial Decision Support System for Urban Streams.”

Gomez, Basil. 1991. “Bedload Transport.” *Earth Science Reviews* 31(2): 89–132.

Gran, Karen B. et al. 2013. “Landscape Evolution, Valley Excavation, and Terrace Development Following Abrupt Postglacial Base-Level Fall.” *Bulletin of the Geological Society of America* 125(11–12): 1851–64.

Hassan, Marwan A. 1990. “Scour, Fill, and Burial Depth of Coarse Material in Gravel Bed Streams.” *Earth Surface Processes and Landforms* 15(4): 341–56.

Hassan, Marwan A., Michael Church, and Philip J. Ashworth. 1992. “Virtual Rate and Mean Distance of Travel of Individual Clasts in Gravel-bed Channels.” *Earth Surface Processes and Landforms* 17(6): 617–27.

Hassan, Marwan A., and Peter Ergensinger. 2003. “Use of Tracers in Fluvial Geomorphology.” In *Tools in Fluvial Geomorphology*, eds. Mathias G. Kondolf and Hervé Piégay. John Whiley & Sons Ltd., 397–423.

Helley, Edward, and Winchell Smith. 1971. “Developmeny and Calibration of a Pressure-Difference Bedload Sampler.” *US Geological Survey*.

Hicks, Murray, and Basil Gomez. 2003. “Sediment Transport.” In *Tools in Fluvial Geomorphology*,.

Hoover, Mackin J. 1948. “Concept of the Graded River.” *Bulletin of Geological Society of America* 59: 463–512.

Houbrechts, G., Y. Levecq, V. Vanderheyden, and F. Petit. 2011. “Long-Term Bedload Mobility in Gravel-Bed Rivers Using Iron Slag as a Tracer.” *Geomorphology* 126(1–2): 233–44. http://dx.doi.org/10.1016/j.geomorph.2010.11.006.

Knighton, A. David. 1982. “Longitudinal Changes in the Size and Shape of Stream Bed Material: Evidence of Variable Transport Conditions.” *Catena* 9: 25–34.

———. 1999. “The Gravel-Sand Transition in a Disturbed Catchment.” *Geomorphology* 27: 325–41.

Koshiba, Takahiro et al. 2018. “Application of an Impact Plate – Bedload Transport Measuring System for High-Speed Flows.” *International Journal of Sediment Research* 33(1): 35–46. http://dx.doi.org/10.1016/j.ijsrc.2017.12.003.

Lane, E.W. 1954. “The Importance of Fluvial Morphology in Hydraulic Engineering.” *United States Department of the Interior Bureau of Reclamation*.

Laronne, J. B., and M. A. Carson. 1976. “Interrelationships between Bed Morphology and Bed-material Transport for a Small, Gravel-bed Channel.” *Sedimentology* 23(1): 67–85.

Leopold, L.B. 1970. “An Improved Method for Size Distribution in Stream-Bed Gravel.” *Water Resources Research* 6: 1357–66.

Leopold, L B, W W Emmett, and R M Myrick. 1966. “Channel and Hillslope Processes in a Semiarid Area New Mexico.” *Geological Survey* 352-G: 193–249.

Liébault, Frédéric et al. 2012. “Bedload Tracing in a High-Sediment-Load Mountain Stream.” *Earth Surface Processes and Landforms* 37(4): 385–99.

López, Raúl, and Javier Barragán. 2008. “Equivalent Roughness of Gravel-Bed Rivers.” *Journal of Hydraulic Engineering* 134(6): 847–51.

Mackin, J. Hoover. 1948. “Concept of the Graded River.” *Bulletin of the Geological Society of America* 5(59): 463–512. papers2://publication/uuid/AC8A6716-22CC-43A5-80AE-59DCB5310A33.

MacVicar, B. J., and A. G. Roy. 2011. “Sediment Mobility in a Forced Riffle-Pool.” *Geomorphology* 125(3): 445–56.

Macvicar, Bruce, Margot Chapuis, Emma Buckrell, and André Roy. 2015. “Assessing the Performance of In-Stream Restoration Projects Using Radio Frequency Identification (RFID) Transponders.” *Water* 7: 5566–91.

Milan, David J. 2013. “Virtual Velocity of Tracers in a Gravel-Bed River Using Size-Based Competence Duration.” *Geomorphology* 198: 107–14. http://dx.doi.org/10.1016/j.geomorph.2013.05.018.

Mosley M.P. 1978. “Bed Material Transport in the Tamaki River near Dannevirke, North Island, New Zealand.” *New Zealand Journal of Science* 21: 619–26.

Muirhead, Christopher Stuart. 2018. “Advances in River Bedload Tracking Technology : Self-Righting Radio Frequency Identification Tracers and an In-Stream Automated Station.” : 109.

Ohmori, Hiroo. 1991. “Change in the Mathematical Function Type Describing the Longitudinal Profile of a River through an Evolutionary.” *The Journal of Geology* 99(1): 97–110.

Papangelakis, Elli, Bruce Macvicar, and Peter Ashmore. 2019. “Bedload Sediment Transport Regimes of Semi-Alluvial Rivers Conditioned by Urbanization and Stormwater Management.” *Water Resources Research*.

Papangelakis, Elli, Christopher Muirhead, Adam Schneider, and Bruce MacVicar. 2019. “Synthetic Radio Frequency Identification Tracer Stones with Weighted Inner Ball for Burial Depth Estimation.” *Journal of Hydraulic Engineering*.

Parker, G. 1991. “Selective Sorting and Abrasion of River Gravel. II: Applications.” *Journal of Hydraulic Engineering* 117(2): 150–71.

Paul, Michael J, and Judy L Meyer. 2001. “Streams in the Urban Landscape.” *Annual Review of Ecology and Systematics* 32(1): 333–65. http://arjournals.annualreviews.org/doi/abs/10.1146%2Fannurev.ecolsys.32.081501.114040.

Phillips, C. B., and D. J. Jerolmack. 2014. “Dynamics and Mechanics of Bed-Load Tracer Particles.” *Earth Surface Dynamics* 2(2): 513–30.

Phillips, R., and J.R. Desloges. 2014. “Glacially Conditioned Specific Stream Powers in Low-Relief River Catchments of the Southern Laurentian Great Lakes.” *Geomorphology* 206: 271–87. http://dx.doi.org/10.1016/j.geomorph.2013.09.030.

———. 2015a. “Alluvial Floodplain Classification by Multivariate Clustering and Discriminant Analysis for Low-Relief Glacially Conditioned River Catchments.” *Earth Surface Processes and Landforms* 40(6): 756–70.

———. 2015b. “Glacial Legacy Effects on River Landforms of the Southern Laurentian Great Lakes.” *Journal of Great Lakes Research* 41(4): 951–64. http://dx.doi.org/10.1016/j.jglr.2015.09.005.

Pike, Leila, Susan Gaskin, and Peter Ashmore. 2017. “Flume Tests on Fluvial Erosion Mechanisms in Till-Bed Channels.” *Earth Surface Processes and Landforms* 270(September 2017): 259–70.

Reid, I., J. T. Layman, and L. E. Frostick. 1980. “The Continuous Measurement Of Bedload Discharge.” *Journal of Hydraulic Research* 18(3): 243–49. http://www.tandfonline.com/doi/abs/10.1080/00221688009499550.

Rennie, Colin D., Robert G. Millar, and Michael A. Church. 2002. “Measurement of Bed Load Velocity Using an Acoustic Doppler Current Profiler.” *Journal of Hydraulic Engineering* 128(5): 473–83. http://ascelibrary.org/doi/10.1061/%28ASCE%290733-9429%282002%29128%3A5%28473%29.

Rice, Stephen, and Michael Church. 1998. “Grain Size along Two Gravel-Bed Rivers: Statistical Variation, Spatial Pattern and Sedimentary Links.” *Earth Surface Processes and Landforms* 23(4): 345–63. http://doi.wiley.com/10.1002/%28SICI%291096-9837%28199804%2923%3A4%3C345%3A%3AAID-ESP850%3E3.0.CO%3B2-B.

———. 2001. “Longitudinal Profiles in Simple Alluvial Systems.” *Water Resources Research* 37(2): 417–26.

Rickenmann, Dieter et al. 2014. “Bedload Transport Measurements with Impact Plate Geophones: Comparison of Sensor Calibration in Different Gravel-Bed Streams.” *Earth Surface Processes and Landforms* 39(7): 928–42.

———. 2017. “Bed-Load Transport Measurements with Geophones and Other Passive Acoustic Methods.” *Journal of Hydraulic Engineering* 143(6): 03117004. http://ascelibrary.org/doi/10.1061/%28ASCE%29HY.1943-7900.0001300.

Schmidt, Karl-Heinz, and Peter Ergensinger. 1992. “Bedload Entrainment, Travel Lengths, Step Lengths, Rest Periods-Studied with Passive (Iron, Mafnetic) and Active (Radio) Tracer Techniques.” *Earth Surface Dynamics* 17: 147–65.

Schneider, Johannes et al. 2014. “Scaling Relationships between Bed Load Volumes, Transport Distances, and Stream Power in Steep Mountain Channels.” *Journal of Geophysical Research: Earth Surface* 119: 333–48.

Schumm, S. A., and R. W. Lichty. 1965. “Time, Space, and Causality in Geomorphology.” *American Journal of Science* 263(2): 110–19. http://www.ajsonline.org/cgi/doi/10.2475/ajs.263.2.110.

Shepherd, R.G. 1985. “Plate Tectonics and Geochemical Composition of Sandstones : A Discussion.” *The Journal of Geology* 93(3): 377–84.

Shields, A. 1936. “Anwendung Der Aehnlichkeitsmechanik Und Der Turbulenzforschung Auf Die Geschiebebewegung.” *Mitt. Preuss* 26.

Shulits, Samuel. 1941. “Rational Equation of River-Bed Profile.” *American Geophysical Union* (2): 622–31.

Simon, Andrew, and Janine Castro. 2003. “Measurement and Analysis of Alluvial Channel Form.” In *Tools in Fluvial Geomorphology*, eds. M. Kondolf and Hervé Piégay. John Whiley & Sons Ltd., 292–322.

Smith, Gregory H. Sambrook, and Robert I. Ferguson. 1996. “The Gravel-Sand Transition: Flume Study of Channel Response to Reduced Slope.” *Geomorphology* 16: 147–59.

Snow, R. Scott, and Ruby L. Slingerland. 1987. “Mathematical Modeling of Graded River Profiles.” *The Journal of Geology* 95(1): 15–33.

Sterling, Shannon M., and Michael Church. 2002. “Sediment Trapping Characteristics of a Pit Trap and the Helley-Smith Sampler in a Cobble Gravel Bed River.” *Water Resources Research* 38(8): 19-1-19–11.

Thayer, James B., and Peter Ashmore. 2016. “Floodplain Morphology, Sedimentology, and Development Processes of a Partially Alluvial Channel.” *Geomorphology* 269: 160–74. http://dx.doi.org/10.1016/j.geomorph.2016.06.040.

Thayer, James B., R. Phillips, and Joeseph R. Desloges. 2016. “Downstream Channel Adjustment in a Low-Relief, Glacially Conditioned Watershed.” *Geomorphology* 262: 101–11. http://dx.doi.org/10.1016/j.geomorph.2016.03.019.

The Sernas Group. 2013. *Master Environmental Servicing Plan Amendment - Seaton Community*.

United Nations. 1997. “Glossary of Environment Statistics.” Series F(No. 67).

Vázquez-Tarrío, Daniel et al. 2018. “Particle Transport in Gravel-Bed Rivers: Revisiting Passive Tracer Data.” *Earth Surface Processes and Landforms*.

Walsh, Christopher J et al. 2005. “The Urban Stream Syndrome : Current Knowledge and the Search for a Cure.” 24(3): 706–23.

Wilcock, P R, and J C Crowe. 2003. “Surface-Based Transport Model for Mixed-Size Sediment.” *Journal of Hydraulic Engineering-Asce* 129(2): 120–28.

Wolman, M.G. 1954. “A Method of Sampling Coarse River-Bed Material.” *Transactions, American Geophysical Union* 35(6): 951–56.

Wyss, Carlos R. et al. 2016. “Measuring Bed Load Transport Rates by Grain-Size Fraction Using the Swiss Plate Geophone Signal at the Erlenbach.” *Journal of Hydraulic Engineering* 142(5): 04016003. http://ascelibrary.org/doi/10.1061/%28ASCE%29HY.1943-7900.0001090.

Yatsu, Eiju. 1955. “On the Longitudinal Profile of the Graded River.” *American Geophysical Union* 36(4): 655–63.

ZINGG, T., 1935, Beitrag zur Schotteranalyse, Schweizer Miner. Petrog. Mitt., 15, p. 39-140.